NAS 5-462 NEG

ER-4608

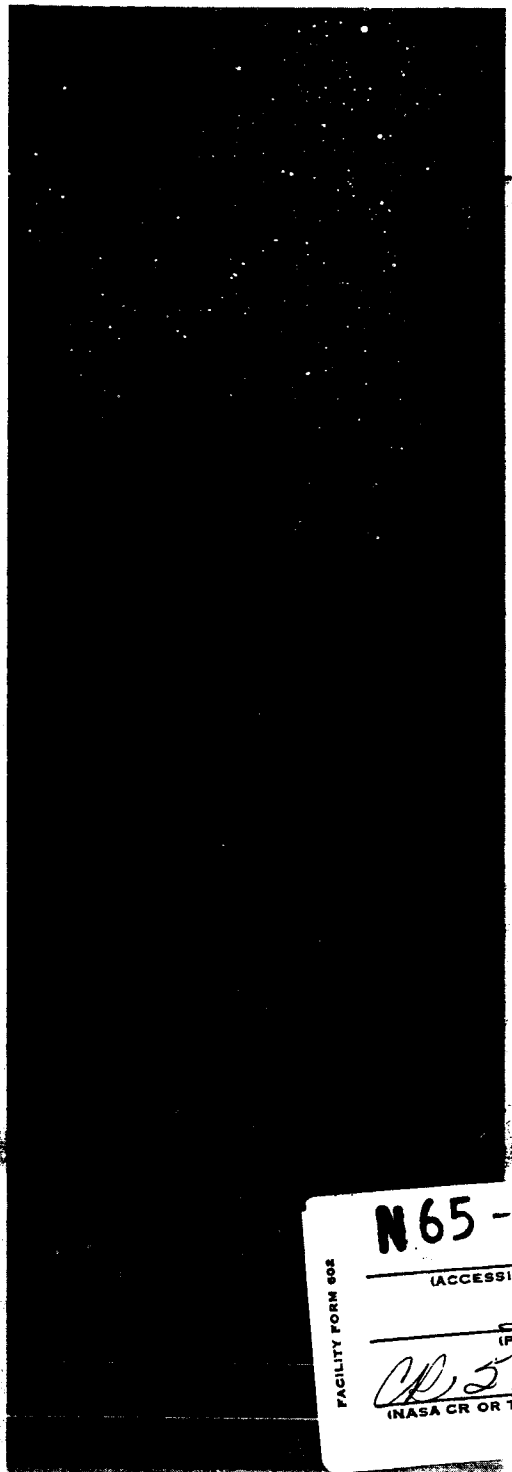

SUNFLOWER POWER CONVERSION SYSTEM

QUARTERLY REPORT

JUNE - AUGUST 1961

TAPCO
a division of
Thompson Ramo Wooldridge Inc.

ER-4608

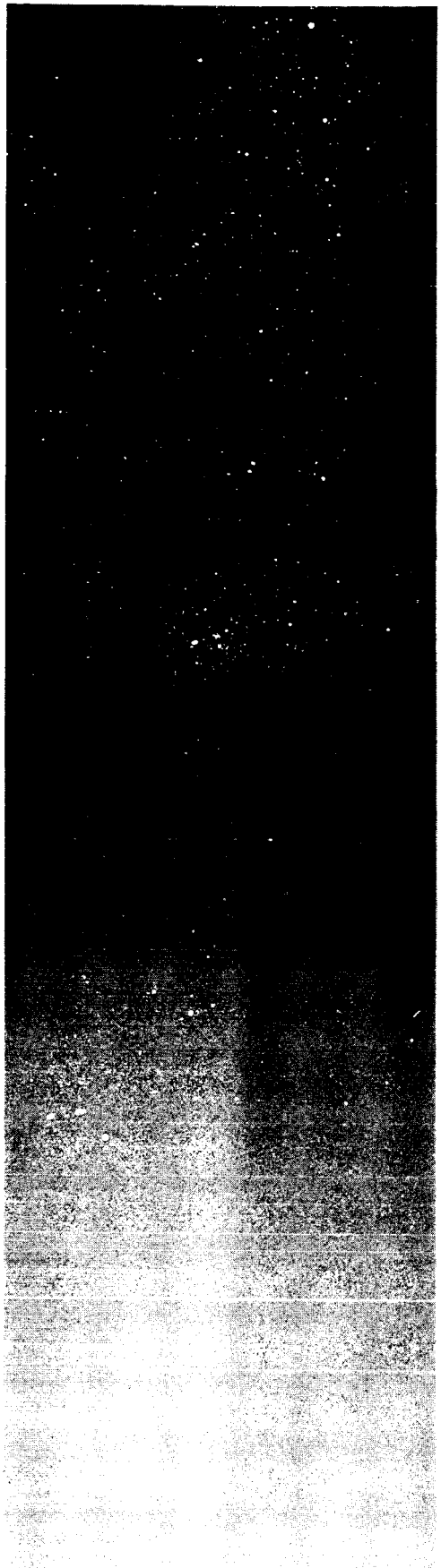

SUNFLOWER POWER CONVERSION SYSTEM

QUARTERLY REPORT

JUNE - AUGUST 1961

TAPCO
a division of
Thompson Ramo Wooldridge Inc.

TABLE OF CONTENTS

LIST OF ILLUSTRATIONS

LIST OF TABLES

1. PROJECT OBJECTIVES

The Sunflower I solar power system objective is to develop a highly reliable power conversion system which is capable of providing a continuous electrical power output from 0.3 to 3 KW in circular earth orbits from 300 to 20,000 nautical miles. The system shall collect the sun's energy in a solar collector and focus this energy in a boiler/heat storage receiver cavity. Mercury shall be heated in the boiler and used in turn to drive the turbine. A directly coupled alternator shall produce the desired output power and the rotational speed of the unit shall be monitored by a parasitic load frequency sensing control. The system shall be capable of operation in all earth orbits between 300 and 20,000 nautical miles and withstanding orbital transfers which require ± 1 g force in any direction. The system shall be delivered in three years and shall have demonstrated at least 90-days endurance capability. A one-year endurance capability shall be demonstrated in four years.

II. PROJECT OBJECTIVES FOR THE REPORTING PERIOD OF JUNE 1, 1961 TO SEPTEMBER 1, 1961

In the last quarterly progress report the following objectives were listed for the current reporting period:

Parametric evaluation of the boiler as a function of boiling pressure and flow will be used to define component requirements and system parameters as determined by system off-design performance. The analysis will add refinement to previous work by incorporating boiler characteristics based upon advanced local heat transfer and pressure drop data.

Checkout of the Auxiliary Mercury Test Rig and installation of the argon inerting systems will be completed. Testing of the condenser, boiler and CSU will be conducted. Initial checkout testing of the C-210 vibration equipment will be completed. Vibration environmental testing of the one-fourth scale fixture will be conducted.

The power conversion system will be released for fabrication.

Test planning and coordination with component personnel will continue. Single panel solar testing will be continued with emphasis placed on obtaining performance data on preprototype collector panels; a variable aperture water-cooled calorimeter will be used to obtain the desired performance maps.

Vacuum deposition of aluminum on collector petals will be attempted and various combinations of filament placement, absolute vacuum, and exposure time will be tried to obtain uniform coatings.

Boiler/heat storage activity will be concentrated on conducting preprototype 1-A component testing and completing the fabrication of preprototype boiler No. 1-B. As data is obtained from testing, it will be factored into the prototype boiler design.

Condenser preprototype testing will be conducted and data factored into design details of the prototype condenser. Dynamic testing will be conducted on several different liquid-vapor interface control devices. Assembly of the prototype condenser will be initiated.

Final assembly and installation of the CSU in the test rig will be completed. The schedule for checkout of the CSU will be dependent upon the duration of condenser and boiler tests.

Testing of the rotational speed control shall consist of checks with an alternator on the alternator dynamometer and preliminary temperature and environmental testing on the preprototype control contingent upon receipt and installation of the two-phase power supply.

Lithium hydride containment efforts will consist of fabrication of capsules for a hydrogen atmosphere test and a sixth set of capsules for an argon atmosphere test. Analysis of the fifth and sixth sets of capsules will be completed. Several capsules will be tested using special coatings to reduce hydrogen diffusion. Calorimeter and thermal conductivity testing of lithium hydride will be completed.

The hydrogen diffusion activity will consist of tests on Haynes 25 and evaluation of plasma-sprayed and oxidized coatings on stainless steel.

The Inglewood Solar Test Rig and site will be completed and installation of the preprototype collector initiated.

III. PROJECT PROGRESS DURING REPORTING PERIOD

PROJECT MANAGEMENT AND SYSTEM ANALYSIS

System analysis has given primary consideration to boiler off-design deviations resulting from external changes characteristic of an orbital vehicle in a sun-shade and acceleration transient. Under the sun-shade transient the transfer of energy to the system is being accomplished under a variable resistance, being a minimum when the boiler tube wall temperature equals the maximum source temperature of 1250°F. A maximum resistance is experienced at the end of a shade period when the melt line of the energy storage material has progressed the maximum distance from the boiler tube wall.

Preliminary evaluation of these operating variables has been conducted and reported previously. The primary improvement in the latest evaluation has been in the improved, time-dependent boiler performance correlation. With this improved boiler correlation the technique employed in the system evaluation was the matching of component characteristics linearized about their steady state design operating points. The results of this evaluation are shown on Figures 1, 2 and 3 for the system operating in 0 g, + 1 g (forward acceleration along the longitudinal axis) and -1 g respectively. Shown on these figures are curves of the combined boiler feed pump - fixed orifice pressure versus flow characteristics at varying pump inlet pressures. These curves cross two boiler-turbine nozzle characteristic curves. Each of these latter curves is for a fixed boiler length equal to the design value of 157 feet. As labeled, one curve represents these combined characteristics for time = 0 (boiler tube wall temperature equals 1250°F) and time = 70 minutes (boiler tube wall varies with length and is less than 1250°F). These two curves are representative of the end of sun period and end of shade period respectively. The operating points for each of these six operating conditions are shown by the OP. notation on the figures. These operating points are calculated by matching system flow characteristics with the condensing pressure level determined by condenser flow. Additional operating parameters associated with each of these operating points are summarized in Tables 1, 2 and 3. It is noted that the only difficulty appears in the +1 g operating condition. Under these conditions the acceleration head on the liquid line from the boiler feed pump to the boiler decreases boiler inlet pressure level causing decreased working fluid flow. While this decrease is not sufficient to reduce the system power output below the 3 kw requirements, it does result in a low condenser pressure and submarginal net positive suction head conditions at the pump inlet. This system deficiency can be readily eliminated by incorporation of a flow regulator located in the boiler inlet line close to the boiler. With such a regulator, operating conditions under any acceleration environment would be along the selected constant flow at the intersection of the time-dependent turbine nozzle characteristic.

Additional effort has been directed toward increasing the thermal capacity of the compact heat exchangers employed for final condensing and subcooling. As is discussed in later sections of this report, condenser component tests to date have indicated insufficient tolerance of the primary radiator to variations in velocity and outlet quality from tube to tube. The sensitivity to these variables will be increased if the exit quality from the primary radiator is increased. This involves a greater thermal burden on the compact heat exchangers.

STEADY STATE OFF-DESIGN OPERATING CHARACTERISTIC AT 0 G ACCELERATION
VARIABLE INVENTORY WITH INTERFACE MAINTAINED AT PUMP C/L. I = 157 FT.

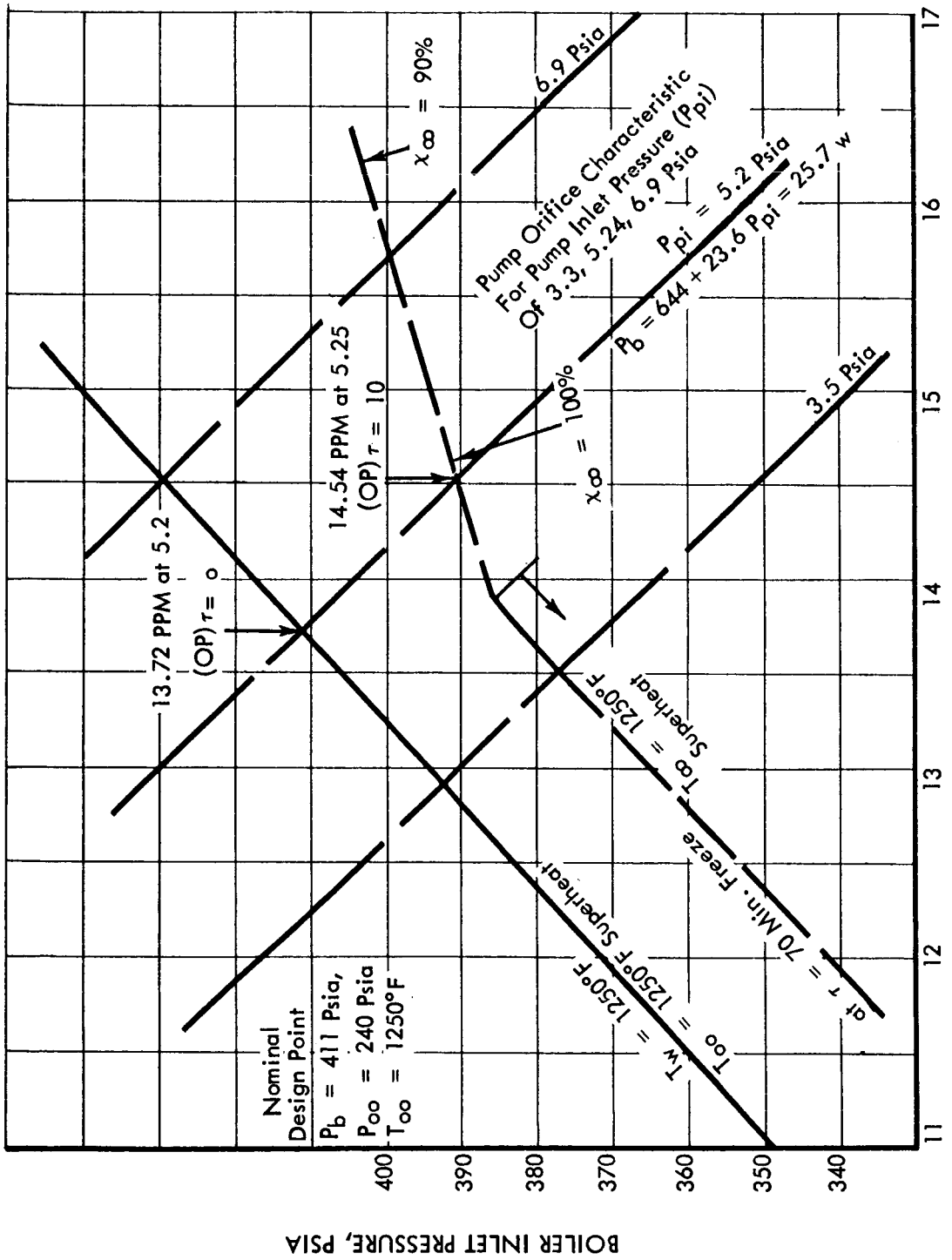

FIGURE 1

STEADY STATE OFF-DESIGN OPERATING CHARACTERISTIC AT (+) 1 G LONGITUDINAL ACCELERATION
VARIABLE INVENTORY WITH INTERFACE MAINTAINED
AT PUMP C/L - PUMP-BOILER HEAD DIFFERENTIAL OF 37 PSI. l = 157 FT.

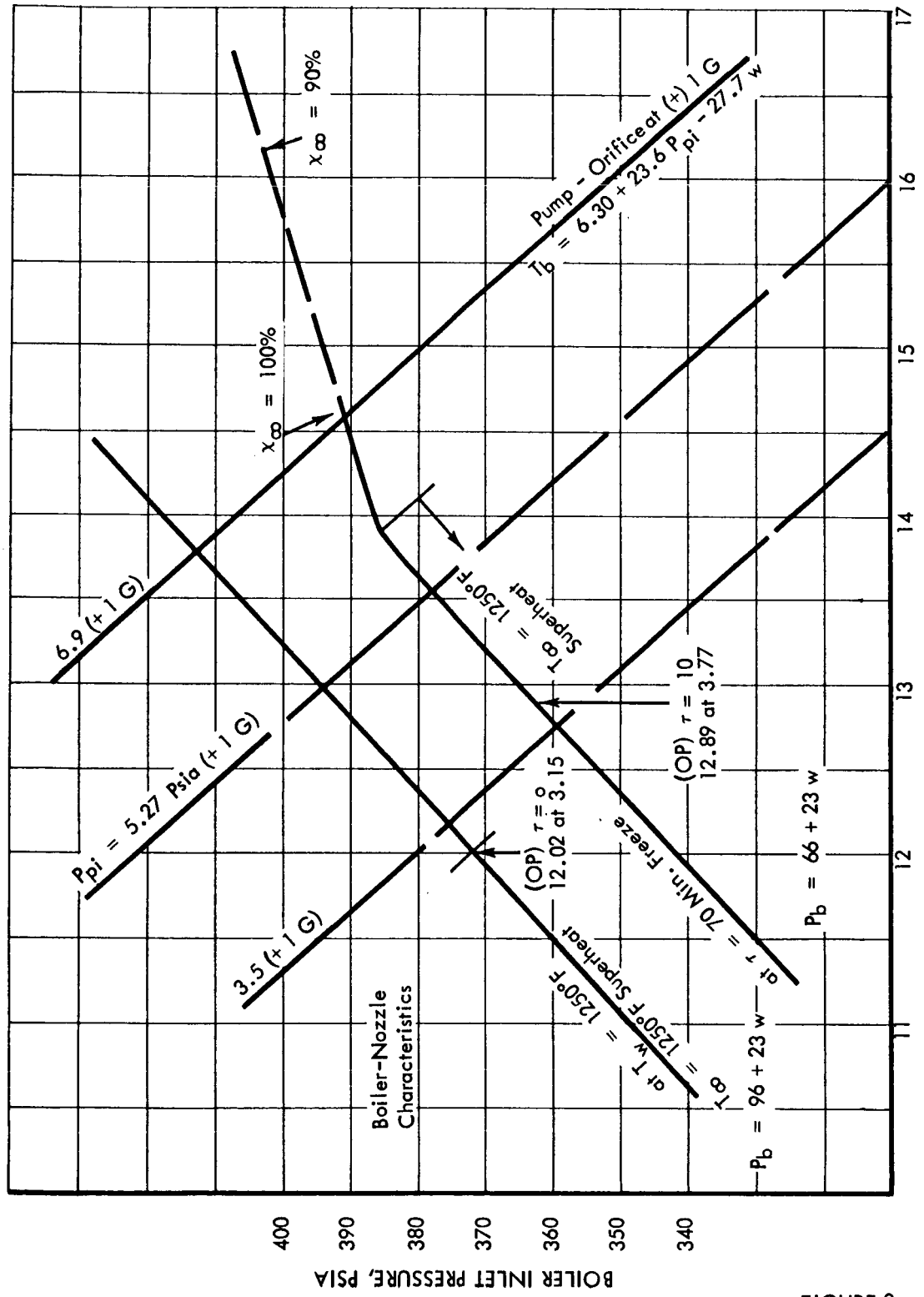

FIGURE 2

STEADY STATE OFF-DESIGN OPERATING CHARACTERISTICS AT -1 G LONGITUDINAL ACCELERATION
VARIABLE INVENTORY WITH INTERFACE MAINTAINED AT PUMP CENTER LINE
PUMP C/L - BOILER HEAD DIFFERENTIAL OF 37 PSI. l = 157 FT.

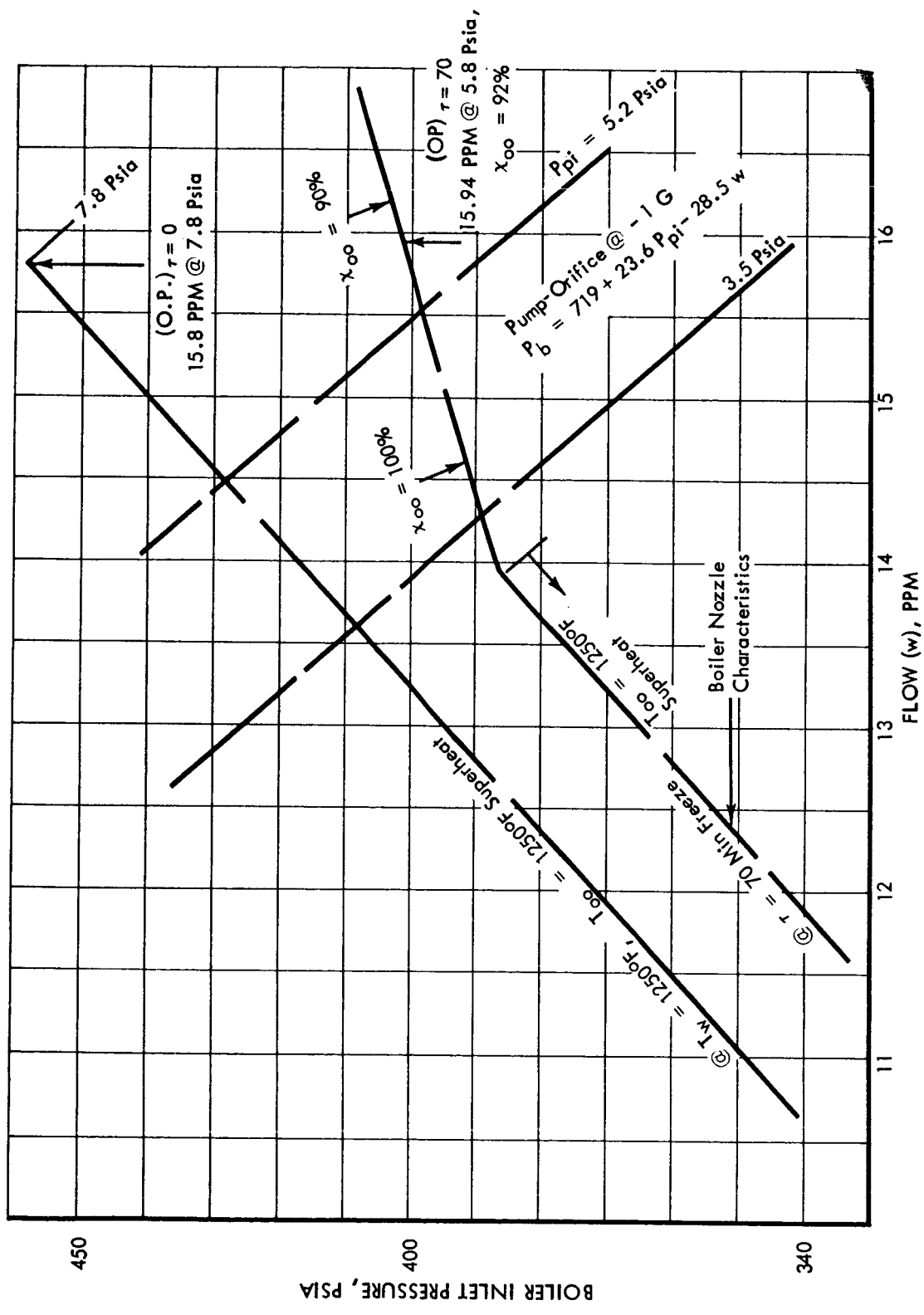

FIGURE 3

TABLE 1

SUMMARY OF BOILER PARAMETER VARIATION

From a Time $\tau = 0$ for Uniform Boiler Tube Wall of 1250°F and at End of 70 Min Shade Period - Boiler Length 157 Ft Fixed Interface (0 G)

	$\tau = 0$	$\tau = 70$
Boiler Inlet - Pressure	411	390
- Temperature	628	628
Boiler Exit - Pressure (P_{oo})	240	240
- Temperature (T_{oo})	1250	1069
Flow - Cycle (w)	13.72	14.54
- Bearing (w_b)	16.00	16.00
Condenser Inlet - Pressure (P_{ci})	7.0	7.3
- Temperature (t_{ci})	605	608
Condenser Exit - Pressure (P_{co})	5.2	5.3
- Temperature (t_{co})	580	583
Pump Inlet - Pressure (P_{pi})	5.2	5.3
- Temperature (t_3)	400	409
- NPSH	4.8	4.9
Subcooler Exit (HE #4) - Temperature (t_{10})	550	553
Turbine Shaft Power ($-Q_t$)	5.0 kw	5.04 kw
Alternator Output	3.5 kw	3.53 kw
Condenser Heat Rejection (Q_c)	29.4 kw	30.3 kw
S/c Radiator Heat Rejection ($Q_{s/c}$)	1.27 kw	0.98 kw

TABLE 2

SUMMARY OF BOILER PARAMETER VARIATION

From a Time $\tau = 0$ for Uniform Boiler Tube Wall of 1250°F and at End of 70 Min Shade Period - Boiler Length 157 Ft Fixed Interface (+ 1 G)

	$\tau = 0$	$\tau = 70$
Boiler Inlet - Pressure	373	363
- Temperature	593	606
Boiler Exit - Pressure (P_{oo})	211	226
- Temperature (T_{oo})	1250	1250
Flow - Cycle (w)	12.02	12.89
- Bearing (w_b)	16	16
Condenser Inlet - Pressure (P_{ci})	4.49	5.35
- Temperature (t_{ci})	568	589
Condenser Exit - Pressure (P_{co})	3.15	3.77
- Temperature (t_{co})	536	551
Pump Inlet - Pressure (P_{pi})	3.15	3.77
- Temperature (t_3)	365	379
- NPSH	2.95	3.51
Subcooler Exit (HE #4) - Temperature (t_{10})	513	525
Turbine Shaft Power ($-Q_t$)	4.62 kw	4.9 kw
Alternator Output	3.18 kw	3.42 kw
Condenser Heat Rejection (Q_c)	25.9 kw	27.7 kw
S/c Radiator Heat Rejection ($Q_{s/c}$)	0.916 kw	0.925 kw

TABLE 3

SUMMARY OF BOILER PARAMETER VARIATION

From a Time τ = 0 for Uniform Boiler Tube Wall of 1250°F and at End of 70 Min Shade Period - Boiler Length 157 Ft Fixed Interface (- 1 G)

	τ = 0	τ = 70
Boiler Inlet - Pressure	459	401
- Temperature	656	632
Boiler Exit - Pressure (P_{oo})	276	250
- Temperature (T_{oo})	1250	1053
Flow - Cycle (w)	15.8	15.94
- Bearing (w_b)	16.0	16.0
Condenser Inlet - Pressure (P_{ci})	10.2	8.2
- Temperature (t_{ci})	645	619
Condenser Exit - Pressure (P_{co})	7.8	5.8
- Temperature (t_{co})	615	589
Pump Inlet - Pressure (P_{pi})	7.8	5.8
- Temperature (t_3)	433	424
- NPSH	7.12	5.2
Subcooler Exit (HE #4) - Temperature (t_{10})	580	558
Turbine Shaft Power ($-Q_t$)	5.32 kw	5.38 kw
Alternator Output	3.95 kw	3.82 kw
Condenser Heat Rejection (Q_c)	33.8 kw	30.4 kw
S/c Radiator Heat Rejection ($Q_{s/c}$)	1.05 kw	1.41 kw

This modification can be made without grossly varying other component requirements in the system. The performance modification to be avoided is increase in flow of the coolant employed to reject heat from the condensate. Since the concept currently employed does not use the total output of the shaft-mounted centrifugal pump, this appears avoidable. Specifically, the total output is now divided into three parallel loops: the jet pump supercharging flow, the bearing lubricant supply, and the boiler feed primary cycle flow. In the present concept, only the latter portion of pump output flow is used as the coolant in the secondary heat exchangers. By using all of the pump output, the coolant flow may be increased from 13.7 lb/min to approximately 44 lb/min. This permits significantly greater heat absorption in the heat exchangers without an excessive temperature rise. This eliminates the requirement for multiple warming and cooling passes through the heat exchangers and secondary radiators.

More analysis and test is required to accurately determine what the primary radiator exit quality should be to gain the required insensitivity to individual tube flow variations. However, the schematic diagram shown in Figure 4 indicates a representative solution based on an increase of the radiator exit quality from 1% to 10%. This concept also succeeds in keeping the secondary radiator temperature high, resulting in an area requirement of 12 ft^2 per side. This can be incorporated with little system modification.

The system structural design has been revised to reflect a requirement for 3 g's lateral acceleration rather than the 1 g value which appears in the contract. This provision and specification has been based on oral statements by NASA. There has also been discussion between NASA and TRW on the advisability of modifying the vibration specifications to which the Sunflower system is currently being designed. Since no specific revised specification has been indentified, the structural design continues to be based on the contract vibration specification.

TEST RIG DESIGN AND FABRICATION

A summary of activity in the test rig area during the reporting period includes the following major events:

a. Final tasks of the test rig assembly, including the auxiliary rig and the test booths, were completed and the rig shakedown accomplished.

b. Rig operation was excellent except for repetitive failure of the auxiliary mercury boiler feed pump. This difficulty appears to have been corrected.

c. The preprototype condenser was installed and tested.

d. The preprototype boiler was delivered to the laboratory and test rig installation initiated.

Details of the above events follow:

REVISED SCHEMATIC - SUNFLOWER

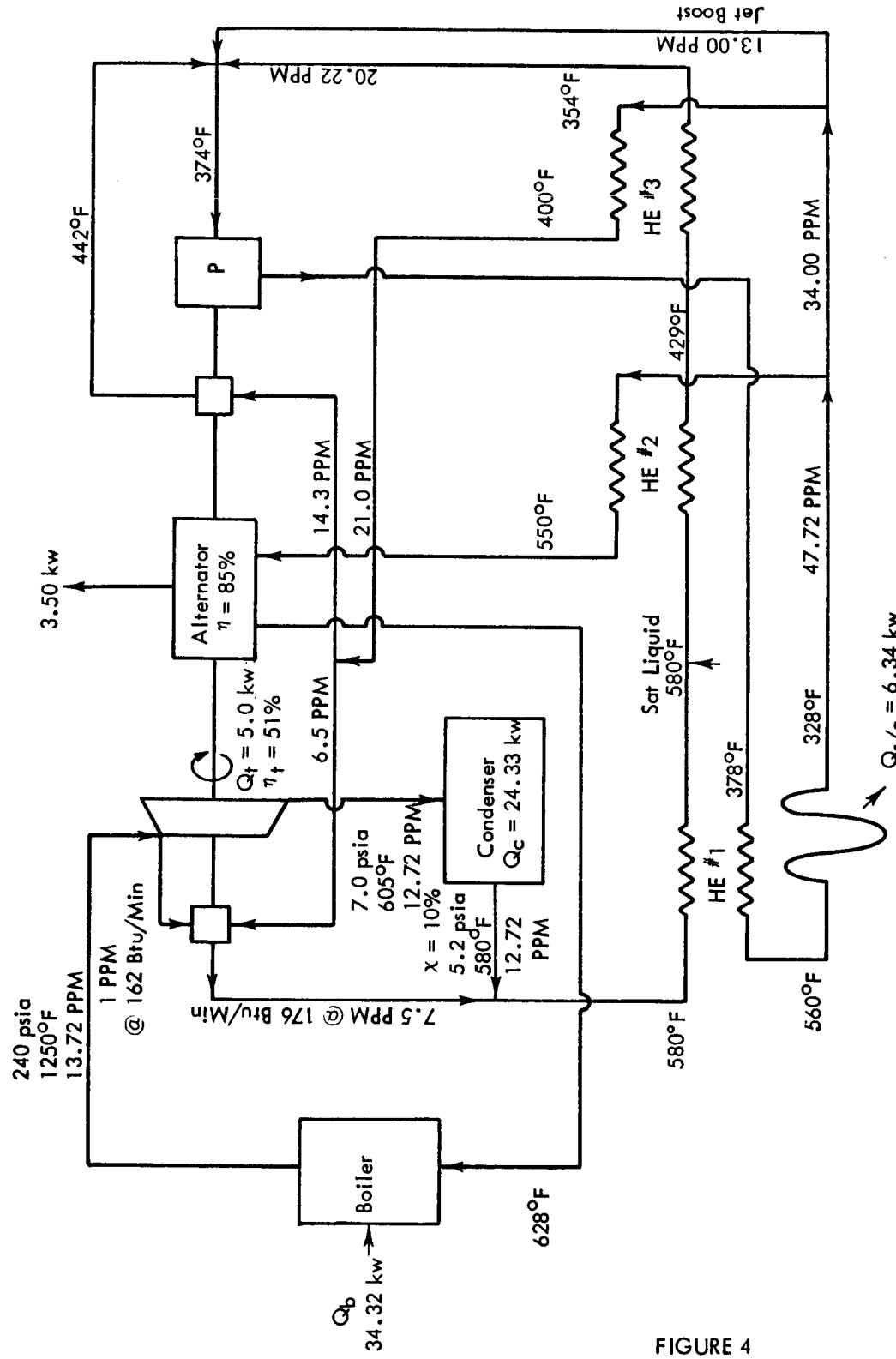

FIGURE 4

During June, air conditioning, ventilation and booth flood lights installations were completed. Final instrumentation, power, and control wiring was also completed.

Prior to installation of the condenser, a 48-hour shakedown run of the auxiliary mercury system was initiated. This is required to perform shakedown operation of the mercury auxiliary system and to precondition the plumbing by circulating boiling and condensing mercury through the system.

Initial operation of the rig was quite successful through the accumulation of approximately 30 hours of operation at design pressure, temperature, and superheat conditions. During this run, rig stability and control were excellent. However, after 30 hours of operation, the auxiliary boiler feed pump failed. The pump was repaired by rework of the impeller and replacement of the seals and bearings in accordance with advice offered by the pump supplier. However, it was found that the pump design did not meet the operating requirements of the rig. During the month of July, two additional failures of the pump occurred after shorter operating periods. After each of these failures further repair and modifications were performed. In early August, it was agreed that the pump should be returned to the vendor for modification in basic design details before further attempts to operate the pump. These modifications were expeditiously accomplished by the vendor and the pump was returned, installed, and operated in the rig in late August. The initial run following this rework was again stopped by evidence of incipient pump failure. However, an additional minor modification was accomplished and the pump now appears to operate satisfactorily.

During the period when the above-described difficulties were occurring, the rig shakedown run was completed and condenser component testing accomplished using a smaller pump owned by TRW. While this smaller pump does not have the capacity required in the testing of the boiler and turbo-alternator components, its capacity was sufficient to allow the shakedown and condenser testing to proceed.

Details of the condenser testing are described in the paragraph on the condenser in the following pages.

The boiler installation was delayed by the heavy effort required in the auxiliary pump evaluation and modification described above and in the heavy effort devoted to the condenser testing. However, the boiler installation did proceed on a second priority basis when possible. Boiler heater power and coolant connections were completed to the test site within the systems booth. The argon inerting system and safety vent installation was largely completed. The boiler was installed on the test fixture pictured in Figure 5.

The fixture designed to support the power conversion system structure at the angle required for vertical loading to simulate 10 g's longitudinal and 3 g's lateral accelerations has been finished. Hydraulic and static loading devices have been designed and are on hand.

The C-210 shaker was delivered during the reporting period and its installation is nearing completion. The shaker is installed on the transport dolly required to move the shaker from the general laboratory pad to the pad located within the system test booth. The hydraulic lifting mechanisms have been assembled and checked out.

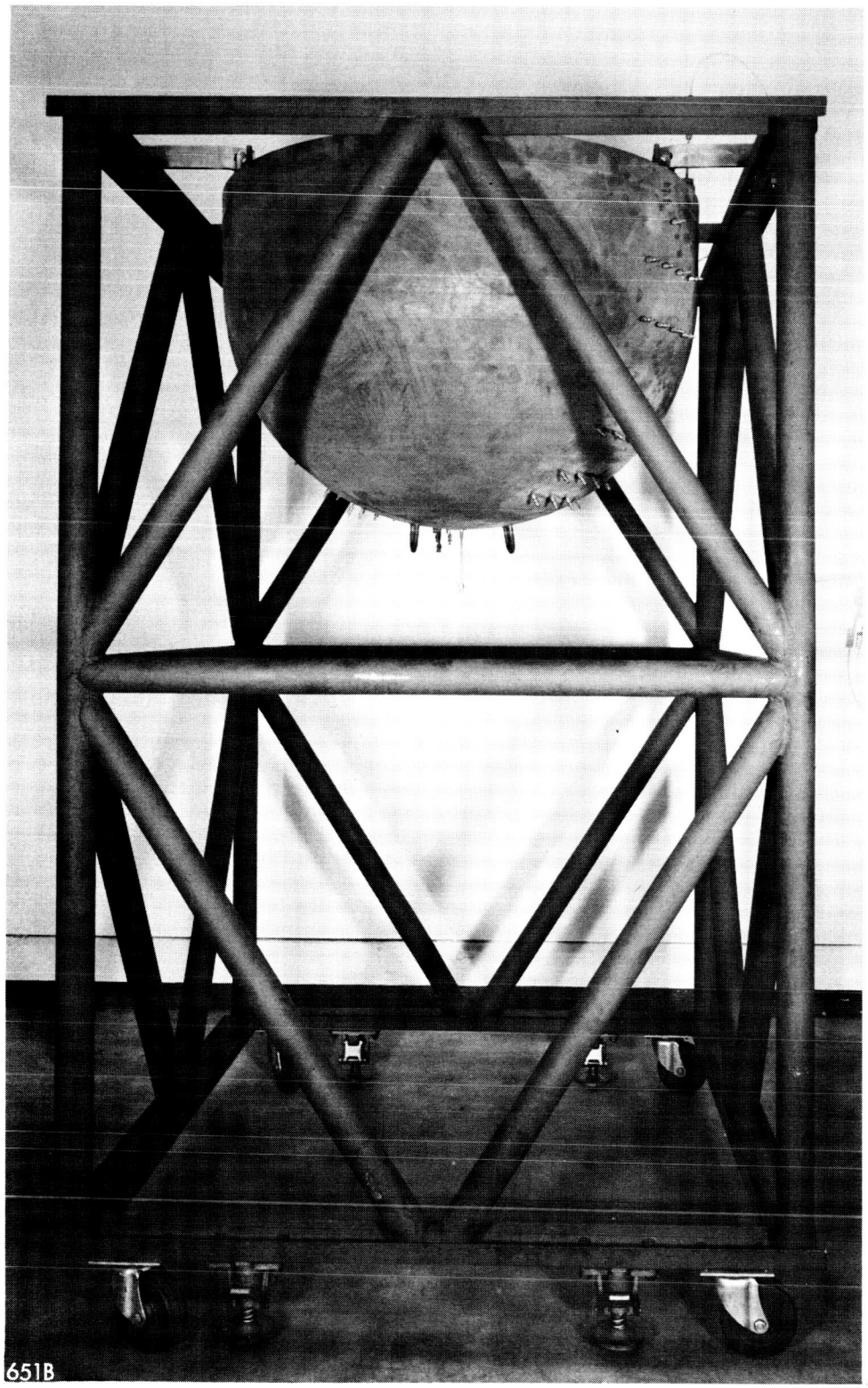

PREPROTOTYPE BOILER IA ON TEST DOLLY

FIGURE 5

The design of fixtures required to transmit vibratory forces from the shaker to the PCS assembly with the limited available vertical distance is proving difficult. Quarter-scale and a half-scale models of the fixture elements have been fabricated of combined magnesium-steel members and subjected to vibration testing to determine resonant frequency and damping characteristics at various load levels. A picture of these beams is shown in Figure 6. The results indicate that the steel web on the fixture beams does not sufficiently increase the loaded resonant frequency and further design effort will be directed toward all magnesium fixtures.

POWER CONVERSION SYSTEM

Design efforts have continued to complete the PCS layout and the bulk of associated detail drawings. Considerable attention has been given to the design of system insulation and preheaters. The preheaters provide the "perculator" inventory return to be employed during ground prestart operations as well as orbital start preheat.

Minor modifications have been made to the system schematic as indicated in Figure 7. The changes which have been made involve refinement of instrumentation and valving requirements. Revisions to the valving have been directed primarily towards insuring that the system startup, operation, and shutdown may be performed during developmental test phases of the system while utilizing either the preprototype inventory charging system with the turbo-alternator package pump or the rig auxiliary pump for inventory transport during startup and operating conditions. The design permits utilization of both pumps in parallel so that system operation may continue through the shifting from one pump to the other.

The system assembly and laboratory transport dolly design has been completed and requests for quotation transmitted to prospective vendors. This fixture, sketched in Figure 8, holds the PCS structure and permits rotation about the axis of symmetry of the structure to facilitate assembly operations. The fixture is provided with wheels and doubles as a transportation dolly to transport the assembled systems around the laboratory area. The hinged base support provides for erection of the system during installation of the assembled systems into the systems development test booth.

SOLAR COLLECTOR

Major attention has been directed toward fabrication of both the heavy duty backup paraboloid to be employed during Inglewood testing and of initial lightweight breadboard panels for use on the single panel test rig. Fundamental inspection and fabrication concept evaluation efforts have also received considerable emphasis.

Immediately after receipt of the fabrication tools and the vacuum metallizing tank last quarter, two lightweight breadboard panels were constructed. These panels are properly defined as breadboard units since they were fabricated from available core and face stock. Due to the unavailability of acceptably high reflectance stock, the face materials were hand polished to improve their specularity. These petals were fabricated to allow experimental

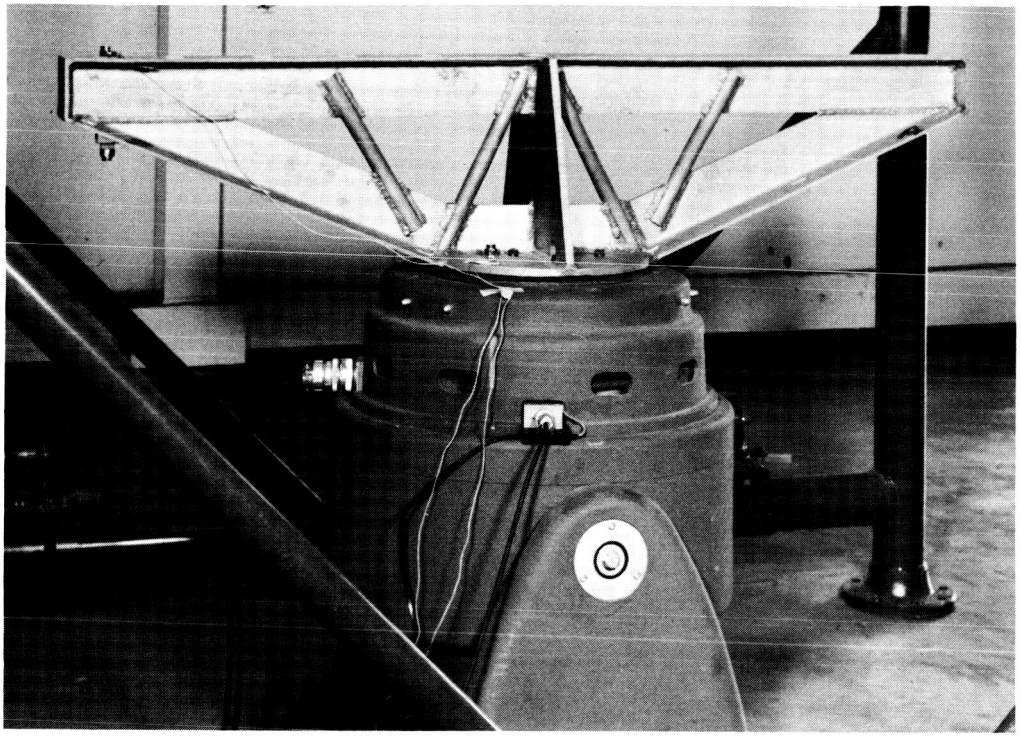

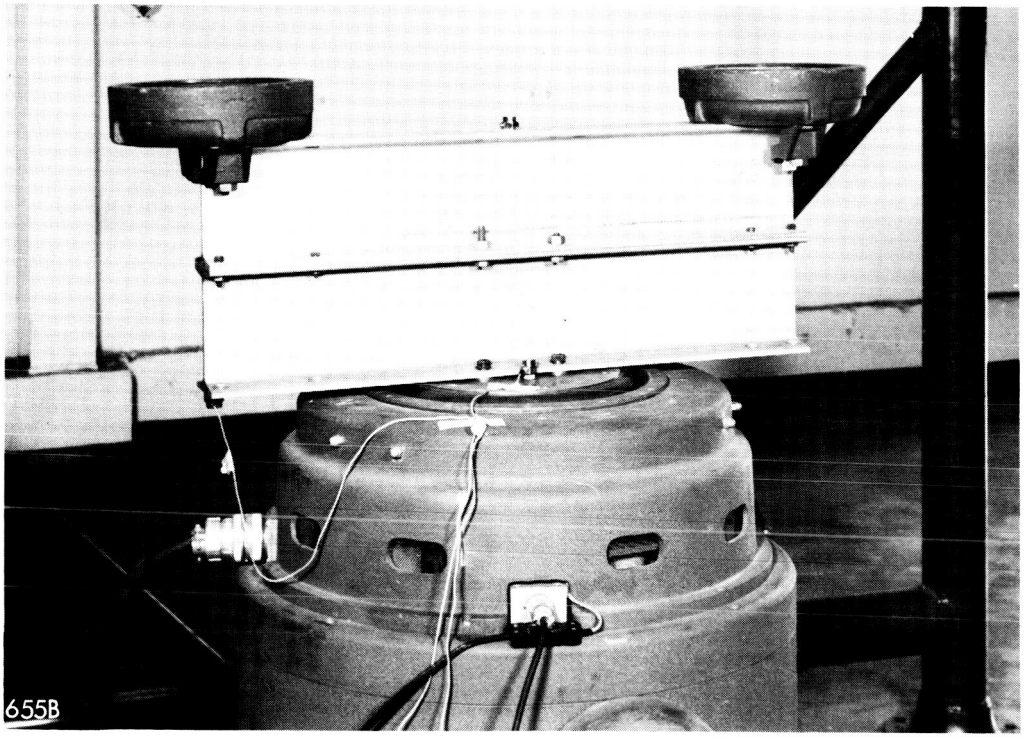

QUARTER-SCALE AND HALF-SCALE VIBRATION MODELS

FIGURE 6

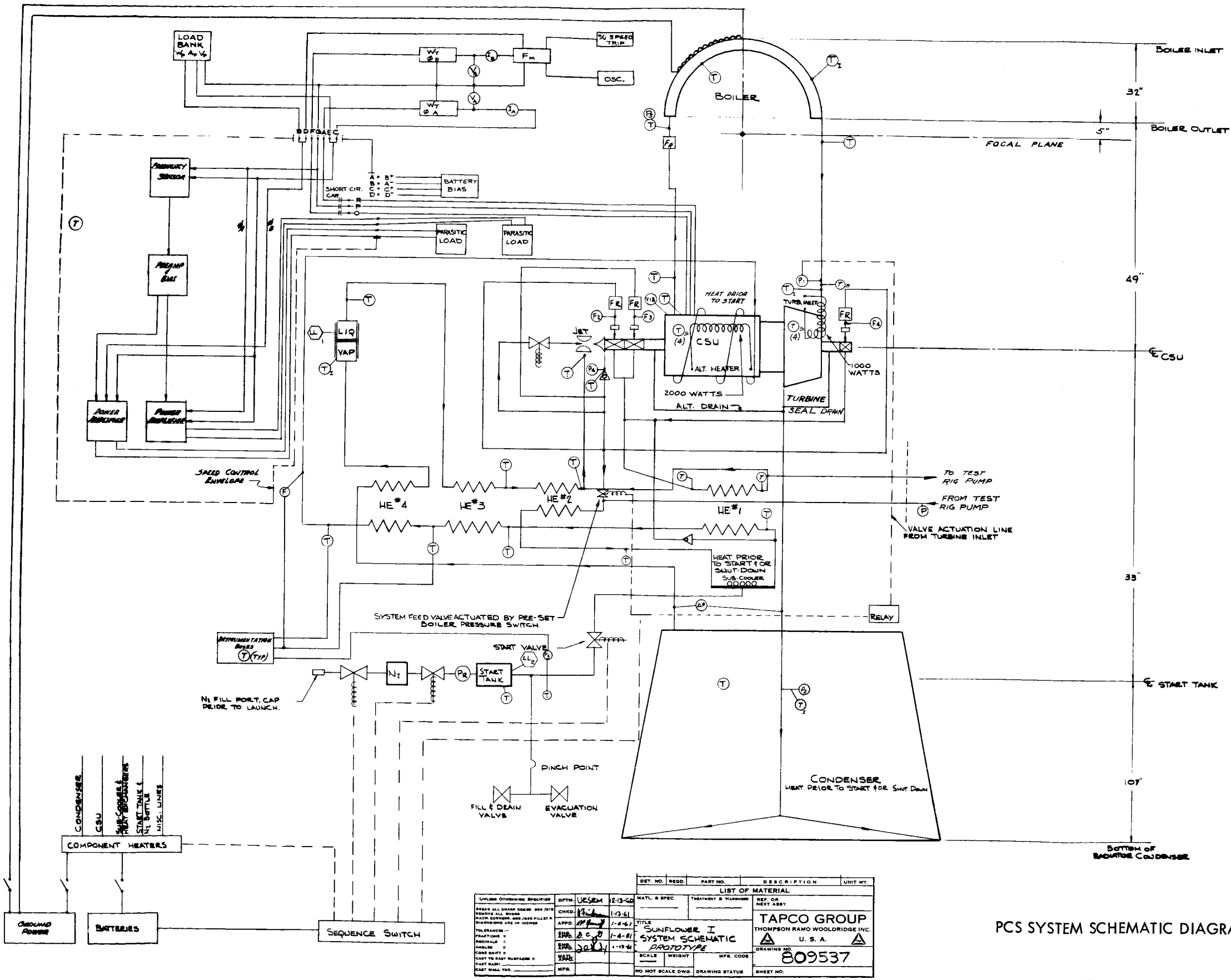

DET. NO.	REQD.	PART NO.	DESCRIPTION	UNIT WT.

LIST OF MATERIAL

UNLESS OTHERWISE SPECIFIED: BREAK ALL SHARP EDGES .005/.015; REMOVE ALL BURRS; MACH. CORNERS .005/.020 FILLET R. DIMENSIONS ARE IN INCHES; TOLERANCES: FRACTIONS ±; DECIMALS ±; ANGLES ±; CODE SHIFT ±; CAST TO CAST SURFACES ±; CAST RADII; CAST WALL THK.

DFTM.	UESEM	12-13-60
CHKD.		1-13-61
APPD.		1-4-61
ENG.		1-4-61
ENG.		1-19-61
MATL.		
MFG.		

MATL. & SPEC. | TREATMENT & HARDNESS | REF. OR NEXT ASSY.

TITLE: SUNFLOWER I SYSTEM SCHEMATIC PROTOTYPE

SCALE | WEIGHT | MFG. CODE

DO NOT SCALE DWG. | DRAWING STATUS

TAPCO GROUP
THOMPSON RAMO WOOLDRIDGE INC.
U. S. A.
DRAWING NO. 809537
SHEET NO.

PCS SYSTEM SCHEMATIC DIAGRAM

FIGURE 7

SYSTEM TRANSPORT AND ASSEMBLY DOLLY

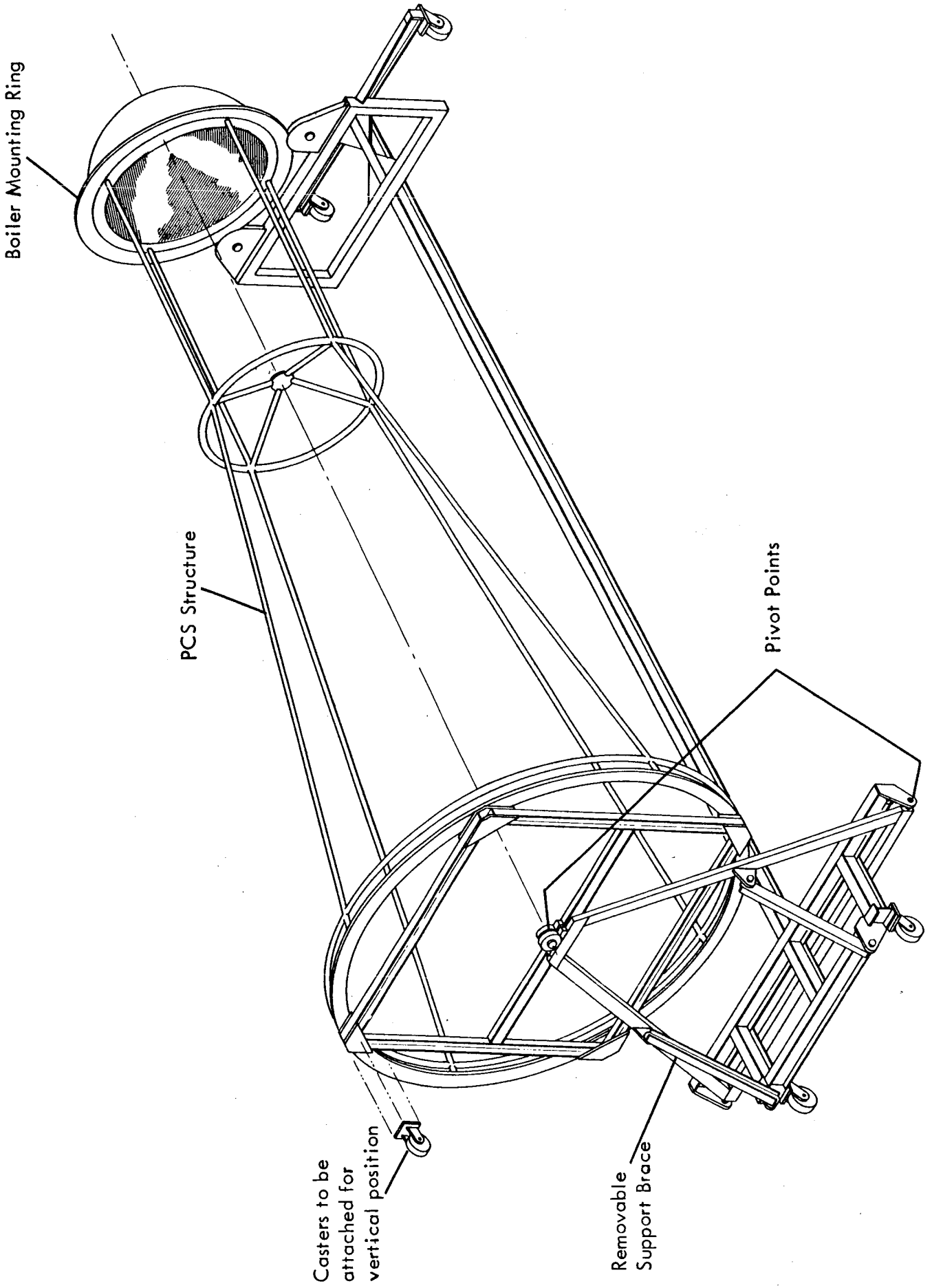

FIGURE 8

efforts to proceed in the vacuum metallizing tank and in the single petal test rig and they suffice for this purpose. The materials availability limitations noted above, however, do influence the performance results obtained on the single panel test rig as discussed below.

After completion of the lightweight breadboard panels, full attention was diverted to supplying the heavy duty panels required for the backup paraboloid structure at Inglewood. This structure employs 24 panels. Since the outer diameter of this structure is 40 feet and the inner diameter 10 feet, each panel is 15 feet long and 5 feet wide at the large end. Twelve of these petals of the type pictured in Figure 9 were delivered to Inglewood on August 30 to permit initiation of their assembly at Inglewood. The remaining 12, along with the 8 backup structural ribs, were ready for shipment at the end of the reporting period.

In the construction of these heavy duty panels, some difficulty was encountered in keeping the honeycomb mark-off within specification limits. Limits are defined only for the outer 4 feet of each petal since this is the only portion of the structure which has optical requirements. The technique employed in the fabrication of the first petal was to coat the fabrication tool with epoxy adhesive prior to lay up of the Fiberglas and cardboard honeycomb structure. It was expected that this coating would conform accurately to the contour of the paraboloid tool and fill in the mark-off areas during the lay-up process. Difficulty was encountered in separating the epoxy adhesive from the fabrication tool after the curing process, and damage to the tool resulted. This was corrected by applying the epoxy adhesive to the petal after removal from the fabrication tool to fill in the out-of-specification mark-off areas. Although this operation was required only for the outer 4 feet of each petal, the time and cost of fabrication was somewhat increased.

The single petal test rig efforts during the reporting period will fall within four areas:

1. Alignment of tracking scope and automatic solar tracking system with reference to the rig structure.

2. Alignment of the breadboard petal with reference to the rig structure.

3. Thermal calibration of the zero loss water-cooled calorimeter.

4. Solar testing of the single petal.

The first two tasks were successfully accomplished and the rig currently has the capability of tracking the sun with a maximum orientation error of 5 minutes.

The calibration of the zero loss water-cooled calorimeter was performed by installing an electrical heater within the calorimeter cavity, and comparing thermal energy absorbed by the coolant with electrical energy supplied to the calorimeter. These tests performed within the laboratory indicated a valid correlation. At the coolant flow rate selected to minimize heat transfer to the environment, it was found that no energy loss correction factor was needed.

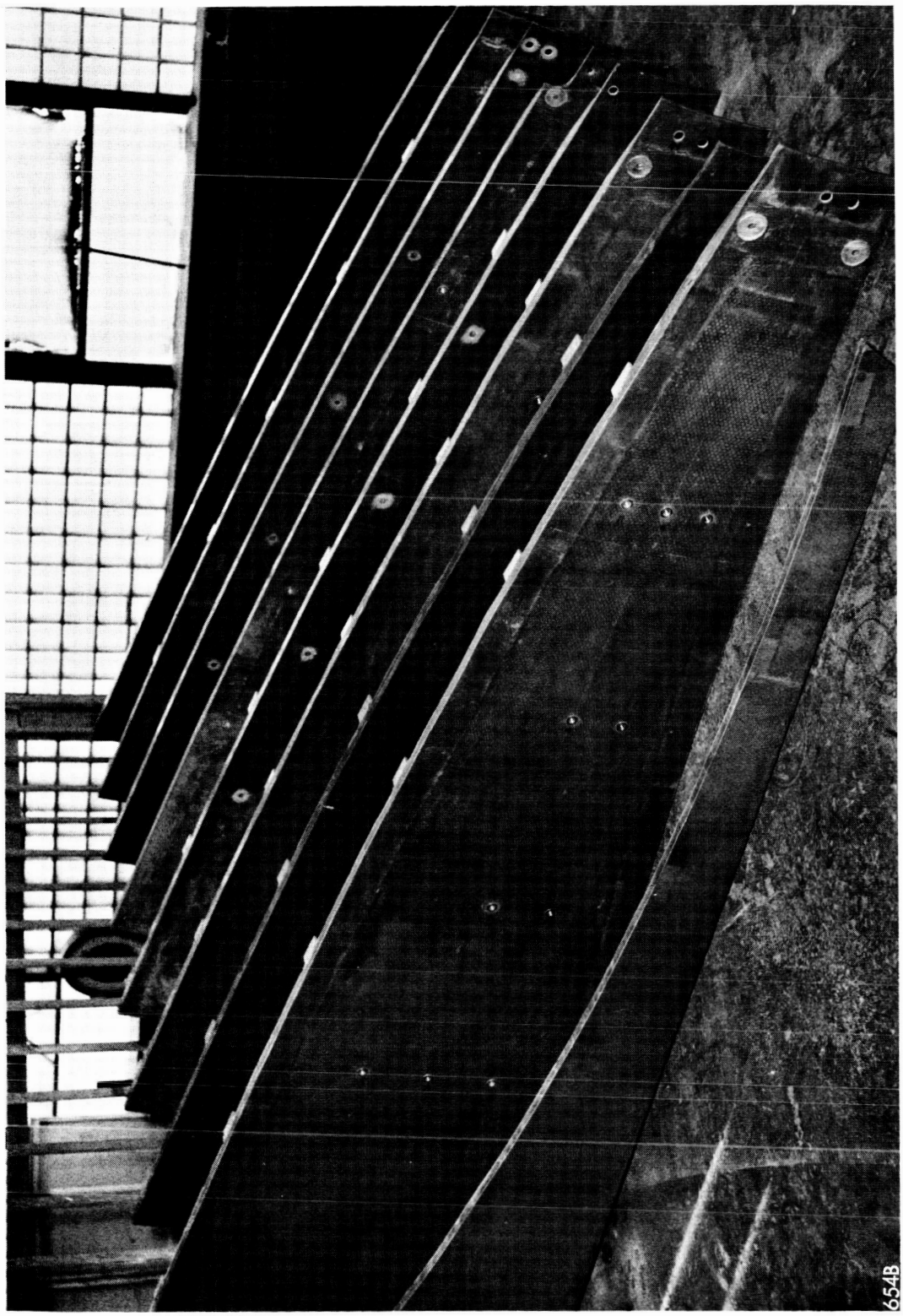

HEAVY DUTY BACKUP PANEL

FIGURE 9

Initial single petal test results achieved an energy efficiency of 63% with the 14.4-inch diameter aperture at the calorimeter. This result was obtained at a zero orientation error. For these tests, the petal is rigidly mounted to the test rig in such a way that errors in gross curvature are eliminated. Since under these conditions no losses result from the honeycomb mark-off, the 63% number compares with a target value of 92% which is the anticipated specular reflectivity of the aluminized petal surface. Investigations are in process to identify the cause of this difference. Visual inspection of the petal indicates that the primary cause is most certainly due to its specular reflectivity. This value is felt to be low for two reasons:

1. The hand polishing which was performed on the optical face of the collector left polish marks. These are visible both by viewing the collector surface, especially when illuminated by bright sunlight, and by viewing the pattern projected to the focal plane when the petal is oriented toward the sun. This pattern is characterized by a diffuse image in the direction normal to the polishing marks.

2. Calorimeter heat loss corrections which may be required for outdoor testing due to forced convection losses in the presence of any breeze.

The contribution of these factors toward the observed collector efficiency will be determined by increasing the temperature instrumentation of the calorimeter and by direct measurement of the specular reflectivity of the test panel. The latter test cannot be performed until completion of the reflectometer described below.

With completion of the vacuum tank installation, process development was initiated on the aluminum and silicon monoxide vacuum deposition processes. This effort is expected to continue into the next quarter. The primary variables being investigated in this effort are filament configuration, aluminum charge per filament, filament spacing, and petal cleaning procedures. The technique employed has been to affix glass plates to the sector as shown on Figure 10.* Each filament was loaded with 0.46 grams of aluminum, the maximum charge it could hold. At operating pressure the charge was preheated at 1000 amps for 2 minutes followed by flashing at maximum filament power - 2650 amps and 11.2 volts for 1 minute. The long flashing time assured complete evaporation of the aluminum.

Transmissivity was determined by the following method. Light was beamed through the portion of the microslide not covered with aluminum. The transmitted light went through a Bausch and Lomb grating monochrometer set at 4000 A exit wavelength. An Aminco photomultiplier microphotometer picked up the exit radiation and was adjusted to read 100%. Then the slide was moved so that the light beam went through the aluminum covered portion. The short wavelength was chosen since a film opaque to this wavelength will also be opaque to longer wavelengths but not vice versa.

*Figure 10 summarizes the results of a typical vacuum deposition operation described here for illustration.

TRANSMISSIVITY VERSUS PETAL LOCATION

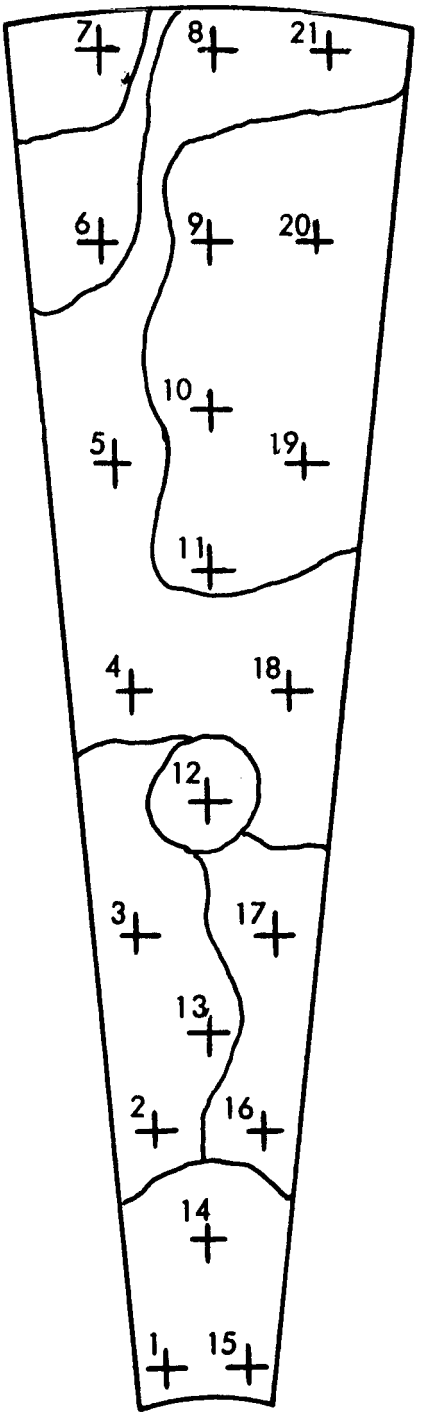

Transmissivity
λ = 4000A

Plate No.	% Transmissivity
1	0
2	0.06
3	0.05
4	0.01
5	0.01
6	0.02
7	0.10
8	0.01
9	0
10	0
11	0
12	0.09
13	0.05
14	0
15	0
16	0.45
17	0.37
18	0.01
19	0
20	0
21	0.01

FIGURE 10

The results are listed next to the diagram on Figure 10. Although the instrument indicated zero transmissivity for several slides, a visual check by looking through the film at the sun revealed that no slide was truly opaque. The sun appeared as a disk of the same brightness as the moon.

With exception of plates 16 and 17, the small amount of transmissivity is of no consequence and could be tolerated. However, since the evaporation time was intentionally longer than optimum, the transmissivity is expected to be higher and variable.

Continuing tests are planned using filaments of a basket configuration, oriented to maximize the evaporating surface in direct view of the petal. It is also planned to try longer filament wires to increase the power capacity of the vaporization. Both these changes should increase the efficiency of mass transfer from the filaments to the target petal, thus increasing the opaqueness of the deposited film. No difficulty is anticipated in achieving the desired surface characteristics with limited continued development in this area.

The deficiency of the hand polishing technique is being corrected in the following manner.

Early contact with the aluminum sheet vendors and specular reflectivity measurements of various products have led to the selection of a desired vendor. An initial shipment received from this vendor, however, did not come up to the specularity standards of the initial test specimens which had led to their selection as a supplier. As a result, this material was returned and effort has been directed towards working out with the vendor more accurate specification definition of the desired material. The unacceptability of the earlier shipment was the reason for hand polishing the first two breadboard petals as noted above. Currently, the vendor is preparing a formal quotation on improved material which will be employed in the fabrication of the petals required for the lightweight panels to be fabricated for further single panel test rig and Inglewood testing.

An additional effort has been the continued evaluation of the thermal distortion characteristics of the Sunflower collector. As previous reports have indicated, tests to date have been restricted to correlating thermal gradients across the thickness of the collector material with adhesive thermal conductivity and the lay-up techniques. During the current reporting period, further testing was directed toward the measurement of actual thermal distortion of cantilevered elements of the collector structure as a function of thermal gradient. The results show that the actual thermal distortion resulting from a given thermal gradient is from one-third to one-half that which would be calculated from an assumption of a homogeneous material with a linear temperature gradient. With this data, sufficient information is available to permit an accurate analysis of the entire paraboloid structure. Such an analysis will define the actual restraints imposed on each individual petal by the currently conceived hinge and lock mechanisms. This investigation will include the influence of different hinge and lock techniques on thermal distortion. Variables which will be evaluated include the employment of additional locking devices at other than the rim position of the petals, and locking devices which impose rotational rigidity as well as circumferential distance rigidity on the petals in the area of the lock.

The final area of effort of the solar collector during the reporting period has been in defining, designing and fabricating hardware required to quickly and accurately inspect each of the petals after fabrication. The procedure which has been selected is schematically shown on Figure 11. The petals will be supported in a manner eliminating the influence of gravity and illuminated with a light source at the focal point. This light will be reflected from the petal through an egg crate grid and onto a photographic plate. The tests of smaller collectors have shown that sensitive qualitative indications of collector optical surface quality can be obtained from the resulting patterns. Photographs of the hardware elements of the inspection system are shown in Figure 12.

CONDENSER-SUBCOOLER

The initial preprototype condenser-subcooler testing was accomplished during the reporting period.

The results of testing have not been fully analyzed to date. However, some qualitative conclusions can be reached.

The condenser radiator was mounted vertically in the test cell and connected to the condenser-subcooler heat exchangers and the secondary radiator. This entire assembly was oriented in the vertically upward position. The installation is shown in Figure 13.

Insulation and electric heaters were installed on the radiator to permit prestart heatup to the design point operating temperature of 600°F with further capability to increase the temperature to the neighborhood of 700°F if desired. The insulation was mounted in such a way that half of it was quickly removable upon startup. By removing half of the insulation and controlling the power applied to the radiator heaters, the radiator could be balanced for proper thermal behavior in the presence of the convective heat transfer existing in the test cell.

An additional detail relevant to the test results is the installation of a drain line in the center of the inlet manifold at the bottom of the radiator. As indicated in Figure 13, the inlet header slopes upward in either direction from the center. Therefore, the central drain was expected to be capable of draining any liquid which accumulated in the inlet manifold.

During initial condenser preheat operation, it was found that temperature instrumentation and individual heating element control was not sufficient to prevent differential thermal expansion between the center radiator structural tube and the parallel tapered tubes. As a result, excessive preheating temperature of the central tube caused sufficient differential thermal expansion to stretch the tapered tubes and cause failure of the outlet tube sheet welds of the two tapered tubes closest to the central tube. This difficulty was corrected by repairing the failed welds and freeing the outlet header from the central tube to allow differential thermal expansion.

SUNFLOWER PETAL INSPECTION RIG

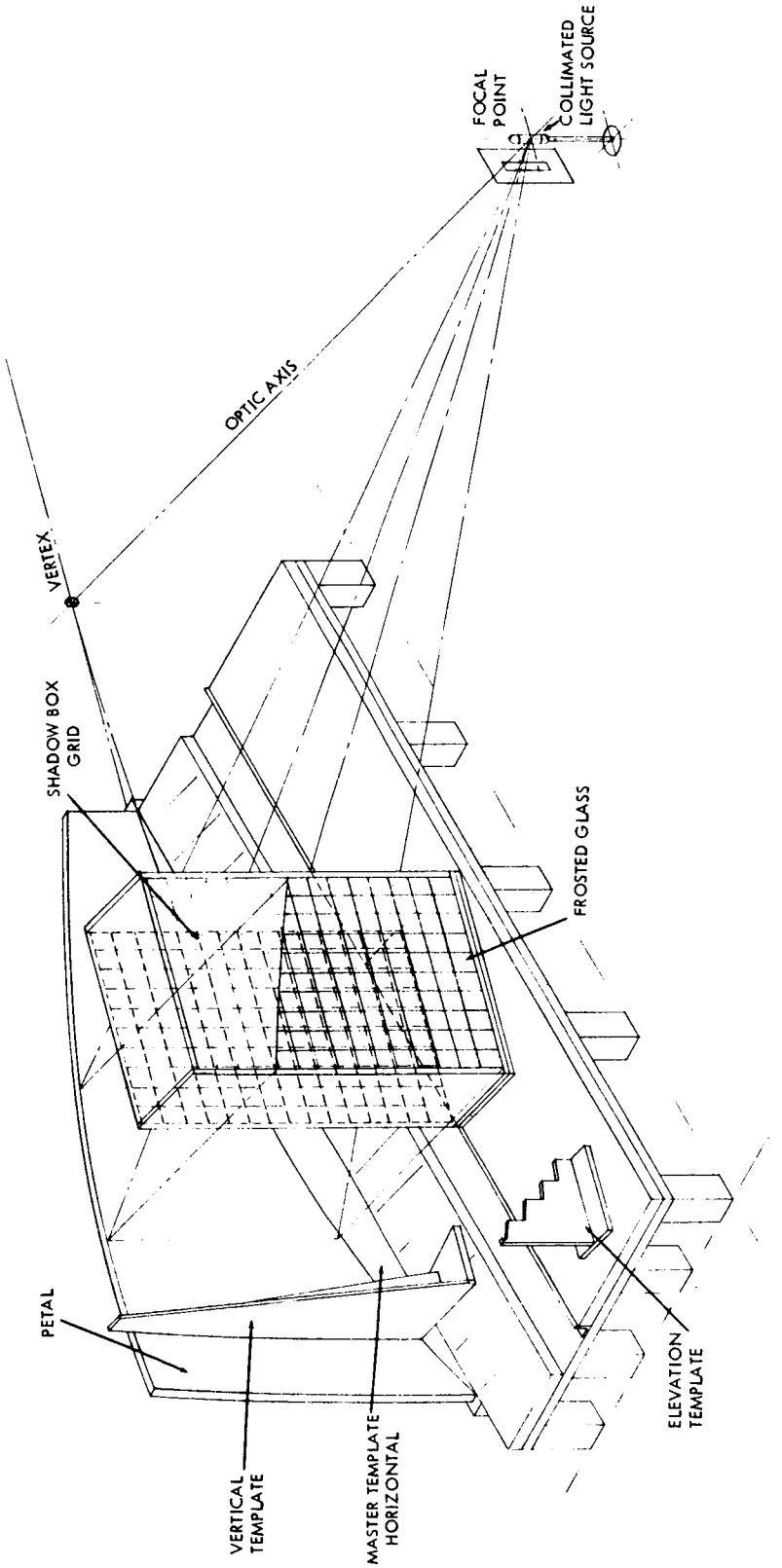

FIGURE 11

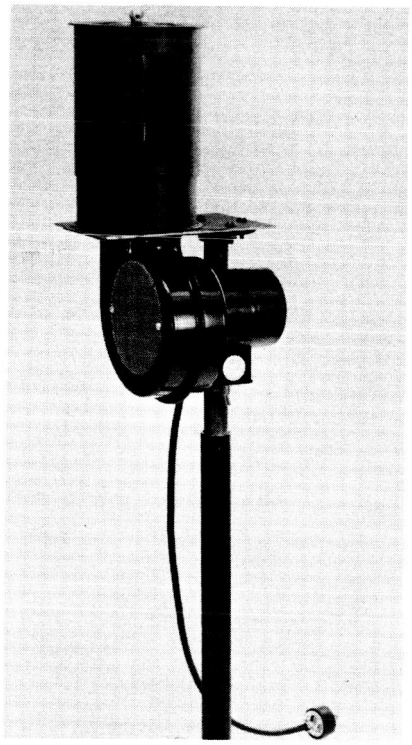

COLLIMATED LIGHT SOURCE

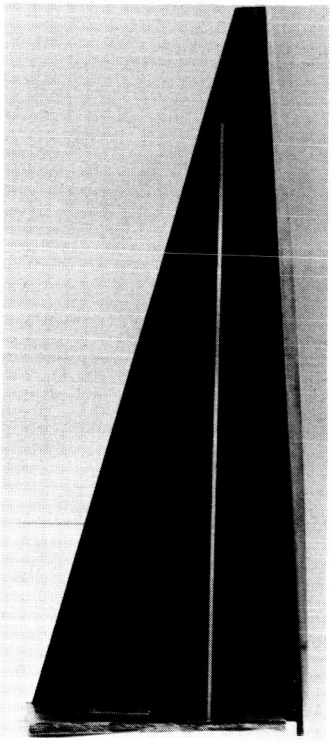

VERTICAL TEMPLATE

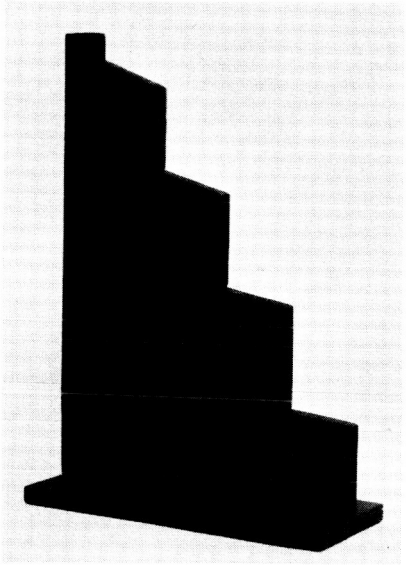

ELEVATION TEMPLATE

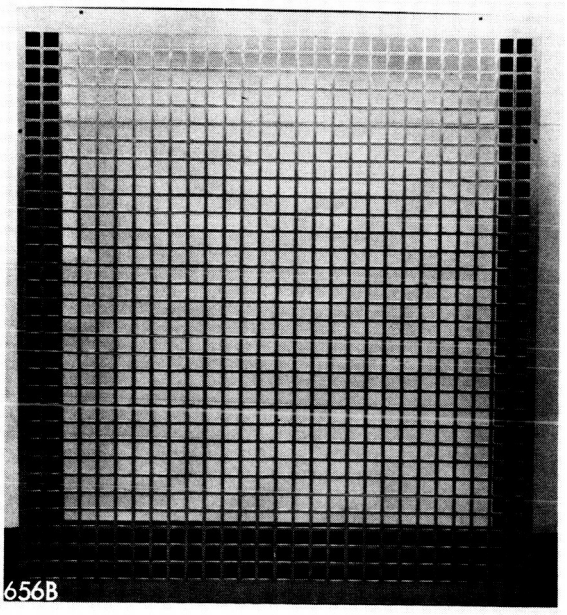

SHADOW BOX GRID

PETAL INSPECTION RIG COMPONENTS

FIGURE 12

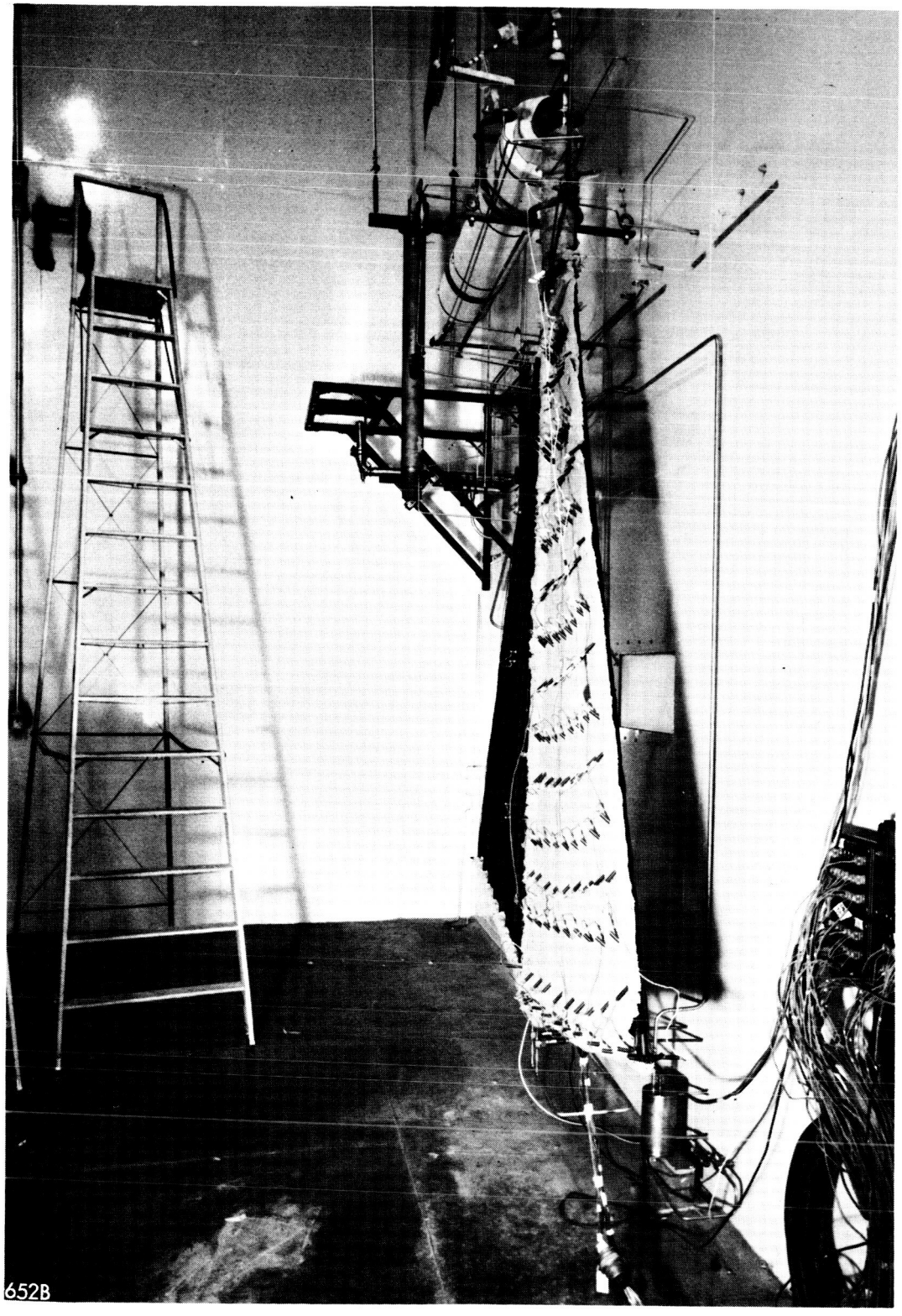

PREPROTOTYPE CONDENSER

FIGURE 13

After this modification, a total of 56 starts was attempted. During each of these attempts it was found that parallel operation of all the tubes was prevented by the buildup and stagnation of a liquid column in the outlet of a portion of the 18 parallel tubes. During these tests, variations in preheat temperature level of the entire radiator, preheat temperature of sections of the tubes, as well as modifications to the liquid draining provisions succeeded in reducing the rate of liquid buildup in the tubes as well as changing the offending tube. Successful operation was not achieved, however.

It is recognized that variation in flow and thermal conditions from tube to tube of the radiator must not be of sufficient magnitude to allow the velocity in any tube to fall below required liquid transport velocity. Such variations must also prevent the quality in any tube from becoming zero. It will be recalled that the design point operating conditions of the radiator are based on an outlet quality of each of the parallel tubes of 1%. At this quality level, the flow from all the tubes is recombined into single line before it is intended that final condensation and subcooling occur. The 1% value appears to be an insufficient margin to prevent reduction of quality to 0% in one or several of the tubes.

As was noted above, the data accumulated during these tests have been evaluated in only a preliminary manner and further testing is planned. However, preliminary conclusions indicate a need to modify the radiator in the following directions:

a. The nominal velocity in the parallel tubes will be increased an amount sufficient to insure that variation of flow conditions will not result in the velocity in any single tube falling below the 60 feet per second value used as the average velocity in the present condenser design.

b. The outlet quality will be increased an amount sufficient to insure that variations in flow and thermal conditions will not allow the quality to fall to 0% in any single tube.

c. The tapered tube outlet dimensions will be increased above the critical interface diameter to prevent the formation of a stable interface in any single tube.

d. Additional details will be evaluated to insure even distribution of liquid transported by the vapor through the inlet manifolding system. The turning requirements imposed on the wet outlet vapor will be reduced.

As a result of these requirements, the test of a modified prototype condenser is planned after completion of the boiler and turbo-alternator component tests.

TURBO-ALTERNATOR

During the reporting period the casting problem reported in the previous quarterly report was solved and nine alternator housing castings are now available for the turbo-alternator and spare parts requirements of the program.

Design activity during the reporting period has continued with the objectives of finalizing the details of heaters, plumbing, and instrumentation installation and of keeping the design consistant with the latest TRW mercury turbo-alternator developmental data.

CSU design was improved by the incorporation of a stress relief operation prior to final machining of all housing castings. This change was made to increase dimensional stability of the package at operating temperatures. Considerable analytical effort was also directed toward the careful evaluation of thermal influences on critical dimensions and stresses within the package. These analyses confirmed that the fits and running clearances of the unit should conform to desired values.

Assembly of the first turbo-alternator has been allowed to proceed more slowly in view of the influence of the condenser test results on the component developmental tests schedule. Since the turbo-alternator component checkout will be performed in the same booth as that employed for condenser testing, its assembly and delivery to the test operation would not expedite its rig installation and test. At the end of the reporting period, the final assembly of the turbo-alternator unit had been initiated and it will be available to the developmental test operation when cessation of condenser testing permits its installation.

ROTATIONAL SPEED CONTROL

The preprototype rotational speed control assembly was completed. Rotational speed control test work during the reporting period included vibration and temperature testing of the components of the prototype unit. These tests include six hours of vibration test of the control transformers at the current vibration specification. This testing was performed for two hours in each of the three major axes of the unit. No degradation of performance of these components was observed. The alternator output capacitors were tested for 150 hours at 125°C with similar absence of measurable performance degradation.

LITHIUM HYDRIDE CONTAINMENT

During the reporting period, the following test occurred:

A. Argon atmosphere capsule furnace

1. Test No. 5 was continued and shut down after 500 hours of operation.

2. Capsules for Test No. 6 were completed, installed, operated, and shut down after 500 hours of operation.

3. Capsules for Test No. 7 were completed, installed, operated, and shut down after 500 hours of operation.

4. Capsules for Test No. 8 were completed, installed, and the tests started.

B. Hydrogen atmosphere capsule testing

1. The hydrogen atmosphere furnace was completed.

2. The first test series in this furnace were performed and shut down after 500 hours of operation.

3. Capsules for the second series of tests were completed, installed, tested, and shut down after 500 hours of operation.

4. The capsules for the third series were completed, installed, and tests initiated. This test was interrupted upon the detection of a lithium hydride leak which was found to stem from defective welds in four molybdenum capsules. After removal of these capsules the test was reactivated and in process at the end of the reporting period.

C. Comparative corrosion testing of lithium, lithium hydride, and lithium-lithium hydride mixtures:

1. The second series of tests, employing three Type 347 stainless steel capsules, were completed after 340 hours.

2. The third set of capsules employing Type 316 stainless steel was completed and the test conducted for a period of 767 hours.

Evaluation of the results of Test No. 4 in the argon environment test series was completed. Evaluation of the results of Tests 5, 6, and 7 remain in various stages of completion at the end of the reporting period. Preliminary data from these reports are included in Tables 4, 5, and 6. The tabular information included for Tests 5 and 6 are preliminary and subject to change.

The four materials used in the construction of the single metal capsules in test group 4 vary greatly in their resistance to lithium hydride. These materials as listed in the order of their ability to resist corrosion under the conditions of the test are: Monoloid Molybdenum, Type 316 stainless steel, A-286 and Hastelloy C premium.

Previous data indicate that AISI 1010 steel and Type 347 stainless steel among others are probably superior to the Type 316 stainless. Metallographic studies have indicated that carbon depletion is common for Type 316 stainless, A-286, Hastalloy C. This observation suggested that the use of metals containing substantial quantities of carbon apparently will not be satisfactory for a container.

As in previous tests, no difference of the severity of attack by lithium hydride has been measured with variation in the purity of hydride over the range of 95% to 98.5%.

TABLE 4

SUMMARY OF TEST CAPSULE RESULTS

FOURTH SET

Material	Capsule Number	LiH Charge, Grams*	Time of Exposure, Hours	Number of Cycles	Weight Change, %	Lithium Hydride After Test, %	Cleaning Procedures	Mode of Corrosion	Depth of Corrosion, Inches	Remarks
Molybdenum	47	3.6**	503	311	-0.07	74.8	C	Intergranular (End Cap and Weld Only)	--	Argon-End caps welded.
Molybdenum	48	3.6	503	311	-0.07	66.2	C	"	--	
Molybdenum	49	3.6	503	311	-0.08	--	C		--	To be continued in Test 5.
Molybdenum	50	3.6**	503	311	-0.08	77.9	C	"	0.005 End Cap 0.002 Weld	
Molybdenum	51	3.6**	503	311	-0.08	--	C			To be continued in Test 5.
Molybdenum	68	--	503	311	-0.105	--	C			
Type 316 SS	62	3.6	1002	621	-0.43	2.3	C	Grain Boundary Penetration	< 0.001	
Type 316 SS	64	3.6	1002	621	-0.42	2.8	C	"	--	Argon-End caps welded.
Type 316 SS	69	3.6	503	311	-0.31	--	H_2			Thermocouple Well-Argon.
Type 316 SS	70	3.6	503	311	-0.42	4.1	H_2	"	< 0.001	Oxidized.
Type 316 SS	71	--	503	311	-0.004	--	H_2			Oxidized.
Type 316 SS	72	3.6	503	311	-0.39	4.9	C	"	--	Oxidized.
A-286	73	3.6	503	311	-0.42	3.8	C	Carbon Depletion	--	Oxidized.
A-286	74	--	503	311	+0.001	--	C			Oxidized.
A-286	75	3.6	503	311	-0.42	2.5	H_2	"	0.001	Oxidized.
A-286	76	--	503	311	+0.005	--	H_2			Oxidized.
Hastelloy C	77	3.6	503	311	-0.45	1.9	C	Carbon Depletion	0.005	Oxicized.
Hastelloy C	78	3.6	503	311	-0.40	1.9	H_2	"	--	Oxidized.
Hastelloy C	79	3.6	503	311	-0.57	2.5	H_2	"	0.0015-0.005	Oxidized.
Type 316 SS-Haynes No. 25	67	3.6	1002	621	-0.40	2.3	C	Haynes 25 Grain Boundary Penetration	< 0.001	Bimetallic
								316 SS Carbon Depletion	0.003	

* 98.5% LiH, 0.066 N_2 Unless Noted

** 95.5% LiH, 0.047 N_2

*** 97.6% LiH, 0.078 N_2

TABLE 5

SUMMARY OF TEST CAPSULE RESULTS

FIFTH SET

Material	Capsule Number	LiH Charge Grams*	Time of Exposure, Hours	Number of Cycles	Weight Change, %	Lithium Hydride After Test, %	Cleaning Procedure	Mode of Corrosion	Depth of Corrosion, Inches	Remarks
Type 316 SS	84	3.6	501	292	-0.31	--	H_2	--	--	Thermocouple well.
Molybdenum	49	3.6	1004	603	-0.15	40.70	C	Intergranular	0.0075	Attack on end-cap only.
Molybdenum	51	3.6***	1004	603	-0.15	45.50	C	Intergranular	--	Attack on end-cap only.
Type 347 SS	88	3.6	3	1	--	--	C	--	--	Oxidized Surface-Failed.
Type 347 SS	89	3.6	501	292	-0.41	3.90	Va	None	--	Electrolytic Chrome Plate.
Type 347 SS	90	3.6	501	292	-0.39	2.98	H_2	Grain boundary	--	
Type 347 SS	91	--	501	292	+0.015	--	H_2	--	--	
Type 347 SS	92	3.6	501	292	-0.50	2.59	C	None	--	
Type 347 SS	93	3.6	498	291	-0.83	43.20	C	None	--	"Solaramic" surface.
Type 347 SS	95	3.6	501	292	-0.39	2.49	C	Intergranular	0.004	Hastelloy W weld attacked.
Type 347 SS	96	3.6	501	292	-0.40	1.29	Va	Intergranular	0.004	Hastelloy W weld attacked.
Type 347 SS	97	3.6	501	292	-0.36	1.68	H_2	Intergranular	0.004	Hastelloy W weld attacked.
Hastelloy X	98	3.6	501	292	-0.43	2.96	C	Carbon Depletion	0.0025	
Hastelloy X	99	3.6	501	292	-0.42	--	C	--	--	To be continued in Group 6.
Hastelloy X	100	--	3	1	--	--	C	--	--	Oxidized Surface-Failed.
Hastelloy X	101	3.6	501	292	-0.41	1.96	C	Carbon Depletion	0.0025	
Haynes No. 25	102	3.6	501	292	-0.29	21.30	C	None	--	Electrolytic Chrome Plate.
Haynes No. 25	103	3.6	501	292	-0.27	21.70	Va	None	--	Electrolytic Chrome Plate.
Haynes No. 25	104	3.6	501	292	-0.26	23.00	H_2	None	--	
Haynes No. 25	105	--	501	292	+0.003	--	H_2	--	--	

*See Table 4

TABLE 6

SUMMARY OF TEST CAPSULE RESULTS

SIXTH SET

Material	Capsule Number	LiH Charge Grams*	Time of Exposure, Hours	Number of Cycles	Weight Change, %	Lithium Hydride After Test, %	Cleaning Procedure	Mode of Corrosion	Depth of Corrosion, Inches	Remarks
Type 316 SS	87	3.6	503	312	-0.23	65.8	C	Grain Boundary	0.0025	Aluminum Dipped.
Type 347 SS	94	3.6	503	312	-0.05	--	C	--	--	Glass-coated. Continued in Test No. 7.
Type 347 SS	141	3.6	503	312	-0.29	10.3	C	None	--	Aluminum Dipped.
Type 347 SS	142	3.6	503	312	-0.27	16.2	C	--	--	Aluminum Dipped.
Type 347 SS	143	3.6	503	312	-0.26	--	C	--	--	Aluminum Dipped. Cont. in Test No. 7.
Hastelloy X	99	3.6	1005	604	-0.40	4.3	C	Grain Boundary	0.0025	Carbon Depletion.
Haynes No. 25	155	3.6	503	312	-0.22	40.0	C	--	--	Etch.
Haynes No. 25	156	3.6	503	312	-0.20	--	C	--	--	Continued in Test No. 7.
Haynes No. 25	157	3.6	503	312	-0.17	53.7	C	Grain Boundary	Hast. W-0.005 19-9-0.0015	Welds attacked. Haynes No. 25 etched.
Haynes No. 25	158	3.6	28	13	--	--	C	--	--	Leaked - defective weld.
Haynes No. 25	159	3.6	28	13	--	--	C	--	--	Leaked - defective weld.
Haynes No. 25	160	3.6	503	312	-0.13	--	C	--	--	Continued in Test No. 7. Mo Insert.
Type 316 ELC	161	3.6	503	312	-0.31	24.6	C	Grain Boundary	< 0.001	
Type 316 ELC	162	3.6	503	312	-0.34	--	C	--	--	Continued in Test No. 7.
Type 316 ELC	163	3.6	503	312	-0.36	7.3	C	Grain Boundary	--	
Type 316 ELC	164	3.6	503	312	-0.36	--	C	--	--	Continued in Test No. 7.
Type 316 SS - Haynes No. 25	151	3.6	503	312	-0.30	15.0	C	None	--	Haynes No. 25 on top.
Haynes No. 25 Type 316 SS -	152	3.6	503	312	-0.31	--	C	--	--	Haynes No. 25 on top. Cont. in Test No. 7.
Haynes No. 25	153	3.6	503	312	-0.27	17.8	C	Haynes 25 - Etched	< 0.001	Type 316 SS on top. Mo Insert.
								Type 316 SS - Deposit	< 0.001	
Type 316 SS -								Insert-G.B.	0.001	
Haynes No. 25	154	3.6	503	312	-0.25	35.4	C	Hs. 25-none.	--	Type 316 SS on top.
								Type 316 SS - Deposit.	--	Mo-1/2 Ti Insert
								Insert-G.B.	0.001	

*See Table 4

Table 7 shows a preliminary tabulation on the results of the first hydrogen atmosphere tests. These tests are being conducted to investigate the variable of decreasing lithium hydride content and increasing lithium content with time. The results of this testing qualitatively support the conclusion, indicated above, that hydrogen loss during a test does not significantly change the corrosion results.

The results of testing in the argon atmosphere through test group no. 4 are now sufficiently complete and explicit that a tentative comparison can be made of the hydrogen permeability of the container materials tested. These permeabilities can be most easily compared by plotting the percentage retained lithium hydride against time as in Figure 14. The greater indicated permeability of Type 316 stainless relative to the Type 347 stainless confirms the difference in the diffusion rates of these materials as reported in the literature.

The lower permeability of the bimetallic capsules probably reflects the lower permeability of the Haynes 25 metal. There is some indication that the diffusion rate is more nearly controlled by that portion of the surface in direct contact with the molten lithium hydride since in this bimetallic test the capsule was oriented in a way to bring the molten hydride in predominant contact with the Haynes 25 portion of the capsule.

Figure 15 shows a plot of permeability versus inversed temperature as compiled from literature and by experimental results. The permeability indicated for the glass-coated diaphrams on Type 303 stainless steel is very attractive. This coating proved to be compatible with a few cycles from room temperature to the 1600°F level; however, subsequent testing for 500 hours between 1200 and 1600°F caused loss of a sound coating.

To correlate these data with system permeability requirements the following calculations are presented:

Assuming that the material used is as good as the curve shown on Figure 15, labeled Aluminized Haynes 25, and further assuming the boiler tube will be at a constant 1200°F, the inner shell at a constant 1600°F, and the outer shell at a constant 1200°F, the following hydrogen losses may be computed.

Outer shell	Area - 30.1 ft^2	
	Thickness - 0.030 in.	
	H_2 loss per year	0.29 lb
Inner shell	Area - 25.1 ft^2	
	Thickness - 0.030 in.	
	H_2 loss per year	7.37 lb
Boiler tube	Area - 19.2 ft^2	
	Thickness - 0.028 in.	
	H_2 loss per year	0.20 lb
	Total H_2 loss per year	7.86 lb

TABLE 7

SUMMARY OF TEST CAPSULE RESULTS

FIRST SET HYDROGEN ATMOSPHERE

Material	Capsule Number	LiH Charge, Grams*	Time of Exposure, Hours	Number of Cycles	Weight Change, %	Lithium Hydride After Test, %	Cleaning Procedure	Mode of Corrosion	Depth of Corrosion, Inches	Remarks
Type 347 SS	109	3.6	472	293	-0.027	--	C	--	--	To be cont. in Group H-2.
Type 347 SS	110	3.6	472	293	-0.025	--	C	--	--	To be cont. in Group H-2.
Type 347 SS	111	3.6	472	293	-0.017	93.15	Va	None	--	
Type 347 SS	112	3.6	472	293	-0.024	--	Va	--	--	To be cont. in Group H-2.
Type 316 SS	113	3.6	472	293	--	--	C	--	--	To be cont. in Group H-2.
Type 316 SS	114	3.6	472	293	-0.029	--	C	--	--	To be cont. in Group H-2.
Type 316 SS	115	3.6	472	293	-0.023	91.44	Va	None	--	
Type 316 SS	116	3.6	472	293	-0.021	--	Va	--	--	To be cont. in Group H-2.
Haynes No. 25	117	3.6	472	293	-0.046	--	C	--	--	To be cont. in Group H-2.
Haynes No. 25	118	3.6	472	293	-0.048	--	C	--	--	To be cont. in Group H-2.
Haynes No. 25	119	3.6	472	293	-0.042	94.44	Va	--	--	Very light etch.
Haynes No. 25	120	3.6	472	293	-0.040	--	Va	--	--	To be cont. in Group H-2.
Hastelloy C	121	3.6	472	293	-0.067	--	C	--	--	To be cont. in Group H-2.
Hastelloy C	122	3.6	472	293	-0.067	90.54	C	Grain Boundary	0.002	Carbon depletion.
Hastelloy C	123	3.6	472	293	-0.057	90.36	H_2	Grain Boundary	0.002	Carbon depletion.
Hastelloy C	124	3.6	472	293	-0.060	90.50	H_2	Grain Boundary	0.002	Carbon depletion.
Type 310 SS	127	3.6	472	293	-0.003	92.88	C	--	--	Deposit (slight).
Type 310 SS	128	3.6	472	293	-0.008	--	C	--	--	To be cont. in Group H-2.
Type 316 SS-Haynes No. 25	125	3.6	472	293	-0.045	91.03	C	--	--	Weld attacked. Deposit on Type 316 SS.
Type 316 SS-Haynes No. 25	126	3.6	472	293	-0.042	--	C	--	--	To be cont. in Group H-2.

*See Table 4

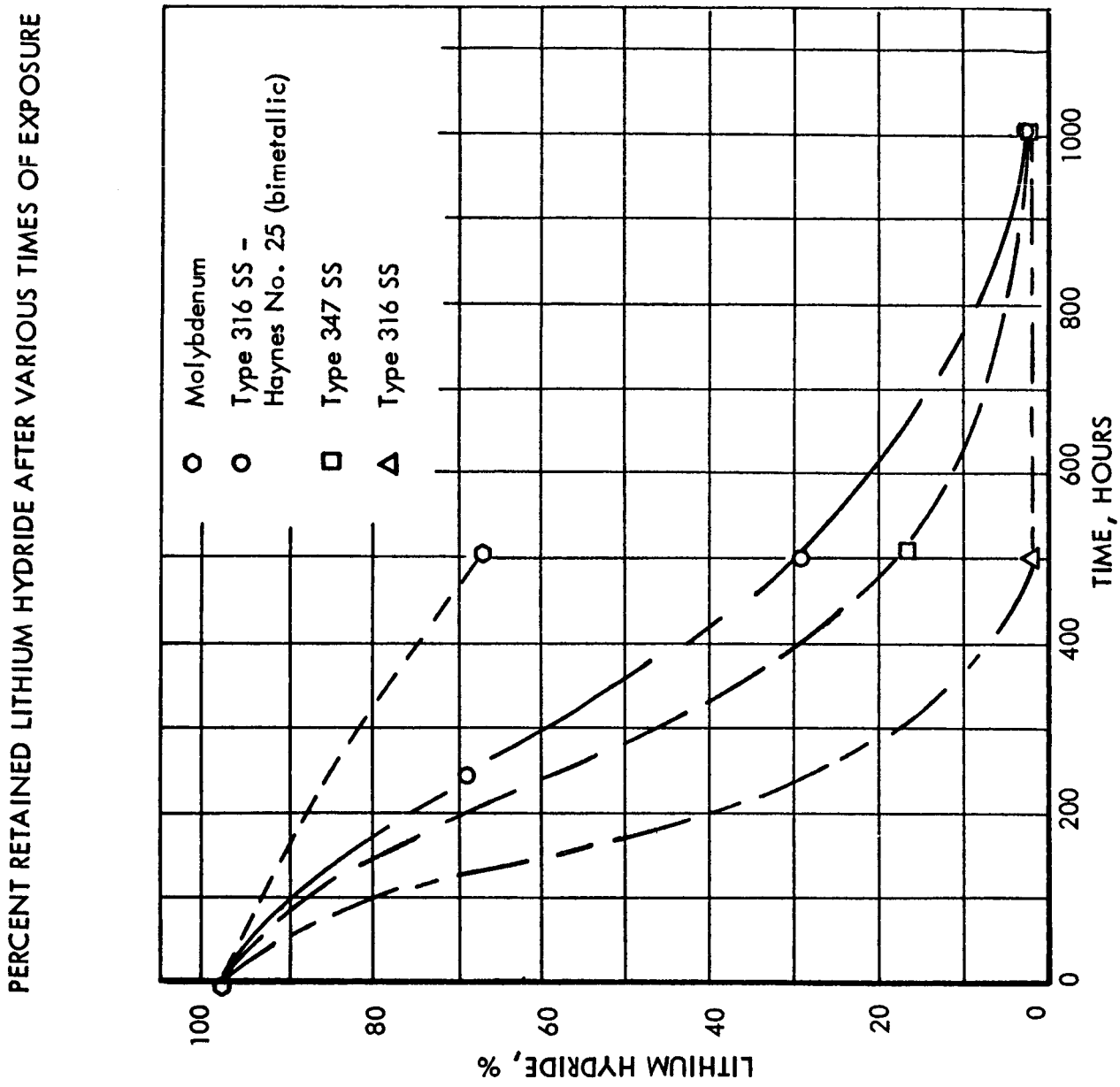
PERCENT RETAINED LITHIUM HYDRIDE AFTER VARIOUS TIMES OF EXPOSURE
Molybdenum
Type 316 SS - Haynes No. 25 (bimetallic)
Type 347 SS
Type 316 SS
LITHIUM HYDRIDE, %
100
80
60
40
20
0
TIME, HOURS
0
200
400
600
800
1000

FIGURE 14

PERMEABILITY DATA FOR VARIOUS MATERIALS

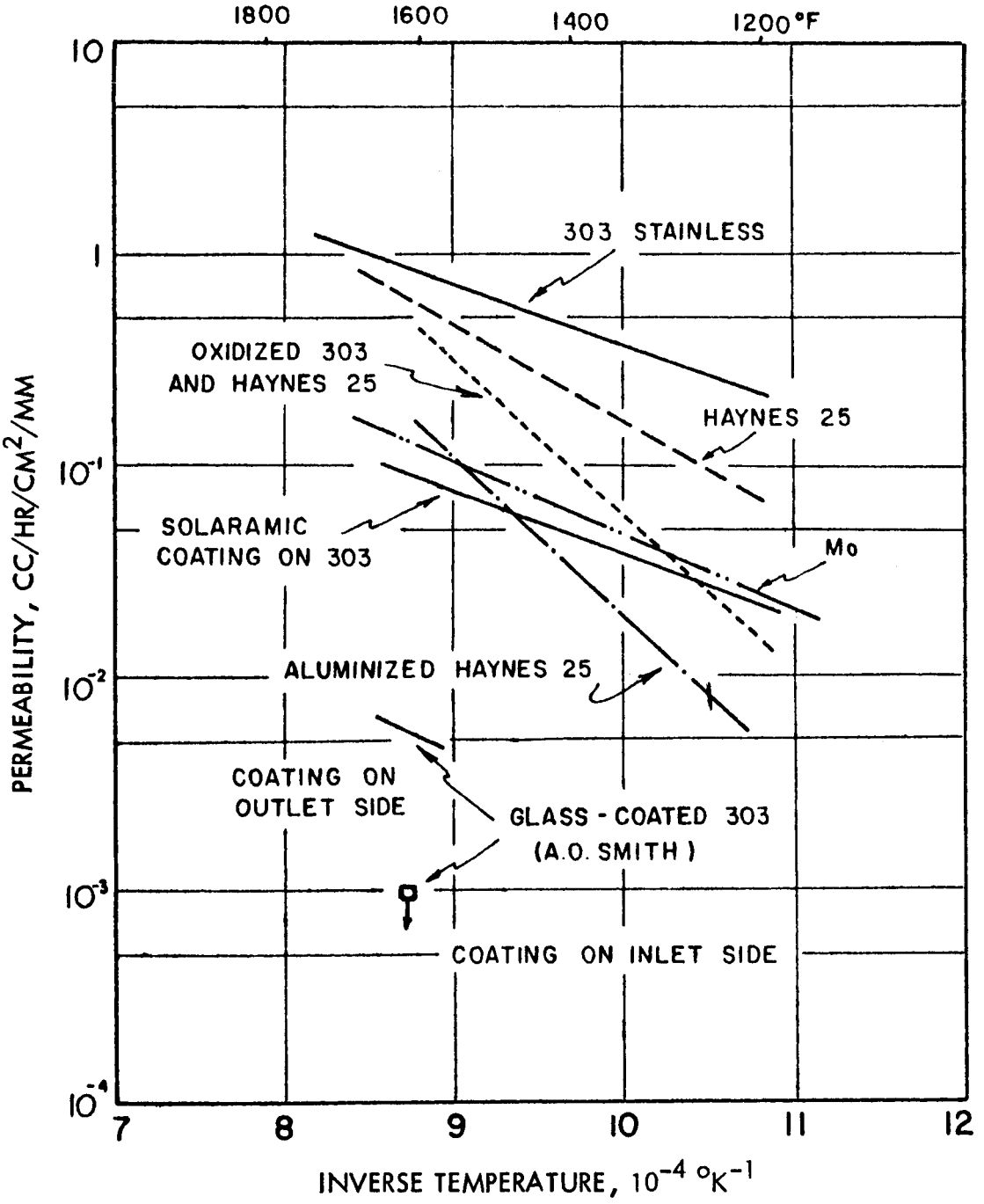

FIGURE 15

Thus, with the measured permeability of aluminized Haynes 25, the hydrogen diffusion could be negated by carrying 8 x 7.86 = 63 pounds of extra LiH.

This calculation serves to identify the problem areas and quantify objectives. The effort will be emphasized in two areas:

1. Further process and coating materials effort will be directed toward achieving a coating compatible with the inner shell environment, having a permeability in the order of 3×10^{-2} $cm^3/hr/cm^2/mm$. This improvement (a factor of 1/5) would reduce H_2 loss to two pounds, representing a more acceptable LiH weight penalty of 16 pounds.

2. Further process and test effort will be conducted to insure that a coating as good as the aluminized Haynes 25 is compatible with the environment of the boiler tube.

The thermal properties experimental evaluation has been completed and a topical report is being prepared.

BOILER/HEAT STORAGE

The preprototype I-A boiler was finished, hydrogen annealed to remove impurities from the internal surfaces, and shipped to the vendor's plant for lithium hydride filling. The filling operation was successfully completed and the unit was returned to the laboratory area at TRW on July 1.

The success of this filling operation was quite gratifying and represents a successful pioneering effort on the part of the Sunflower project. The annular container which forms the preprototype I-A boiler was charged with 140 pounds of lithium hydride.

The preprototype I-A boiler will be used for component tests in the systems test booth of the development and acceptance test rig. Difficulties with the test rig pump and with the test of the preprototype condenser prevented initiation of the test of this component during July. At the end of the reporting period the boiler was being installed and tests were expected to begin during September.

The second preprototype boiler (Model I-B) has been designed and is in final fabrication assembly phases. This unit is fabricated from stainless steel shells identical to those employed in the preprototype I-A model. The I-B boiler also employs a preheater and boiler tube of identical dimension and length as that employed in the first unit. Relatively minor differences in configuration were employed in the two boilers to allow determination of preferred concepts. In particular, the preprototype I-A model employs no heat input fins and has the preheater length located at the apex of the hemispherical container. The preprototype boiler I-B model has the preheater length located at the maximum diameter section near the lower rim and does employ heat input fins. Another innovation of the second boiler is the provision of an expansion volume tank to contain the increased lithium hydride volume resulting from melting. Employment of this chamber permits the complete

filling of the boiler/heat storage unit itself. This permits a comparison of boiler performance in the solid lithium hydride state with and without the voids resulting from the contraction of freezing.

The preprototype I-B boiler is intended to be employed in testing of the PCS-1 system.

Results of the heat input and heat rejection lithium hydride module testing were evaluated. The results are discussed below.

The summary graphical presentation of the heat input results is shown in Figure 16. This is a plot of lithium hydride transport heat flux versus hot wall temperature with and without fins of various spacing. At the internal cavity surface area of present designs, an average heat flux of approximately 10,000 Btu/hr/ft^2 is required. Figure 16 shows that this heat flux may be accomplished without fins if the cavity surface temperature is permitted to increase to 1640°F. This value for the no fin case is sufficiently close to the 1600°F value which has been employed in the Sunflower materials compatibility test work that it holds promise of eliminating fins altogether from the Sunflower boiler. Experimental results obtained from the comparison of the preprototype I-A and I-B boilers will be used to confirm this.

Analytical determinations of the distribution of internal cavity temperature are continuing. Typical results for a specific case in which the internal infra-red emissivity is 0.50 and the solar absorptivity to infra-red emissivity ratio is assumed equal to 1.25 are shown in Figure 17. These assumptions are consistent with published values on unoxidized Haynes 25 surfaces. The results indicate a maximum temperature deviation of 30°F from the directly illuminated areas to the shaded areas of the cavity surface. These calculations will be expanded to account for greater than hemispherical cavity surfaces, since this is the configuration now planned for the lightweight preprototype Model II boiler configuration. These results are preliminary and approximate. However, the results indicate a sufficiently smooth temperature profile that no concerted effort is planned to rigorously calculate these values prior to the time when direct experimental measurements will be possible. This experimental data will be indicated by the solar collector-calorimeter component testing at Inglewood and confirmed by the later high cavity temperature system tests at that facility.

SOLAR TEST RIG

The current status of the solar test site at the TRW Inglewood Plant is indicated by the recent photographs shown in Figure 18. The removable shelter is nearing completion. Retrofit modification on the SPUD rig to be employed in support and tracking of the Sunflower solar collector and system is progressing rapidly and assembly of the heavy duty paraboloid collector support structure was ready to begin at the end of the reporting period.

An updated layout drawing of the solar test rig is included as Figure 19. This presentation is similar to that included in the last quarterly report with the addition of the secondary structure to support the safing tub. The safing tub detail design has not yet been completed

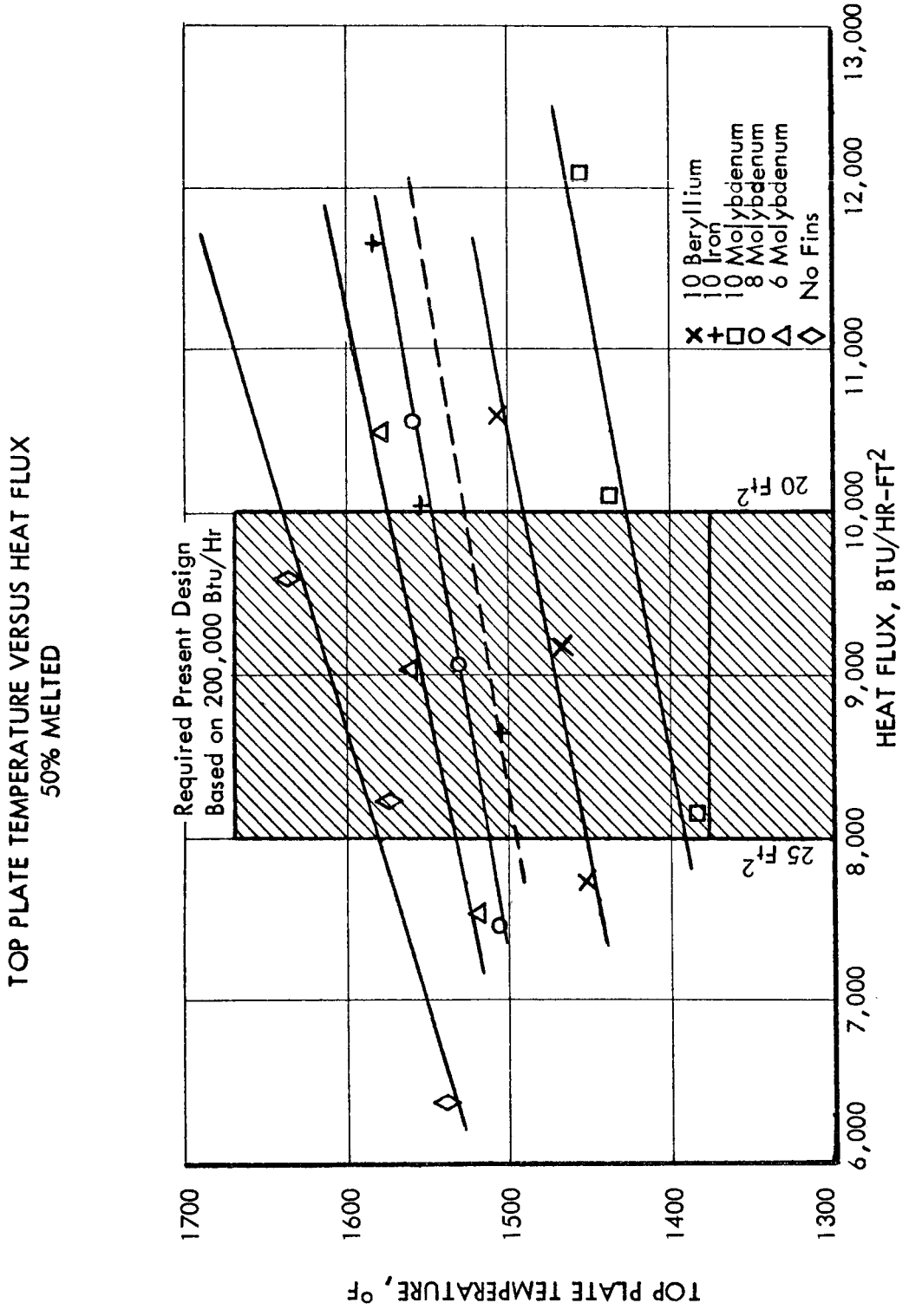
TOP PLATE TEMPERATURE VERSUS HEAT FLUX
50% MELTED
Required Present Design
Based on 200,000 Btu/Hr
20 Ft²
25 Ft²
10 Beryllium
10 Iron
10 Molybdenum
8 Molybdenum
6 Molybdenum
No Fins
HEAT FLUX, BTU/HR-FT²
TOP PLATE TEMPERATURE, °F
6,000
7,000
8,000
9,000
10,000
11,000
12,000
13,000
1700
1600
1500
1400
1300

FIGURE 16

TYPICAL CAVITY SURFACE TEMPERATURE DISTRIBUTION

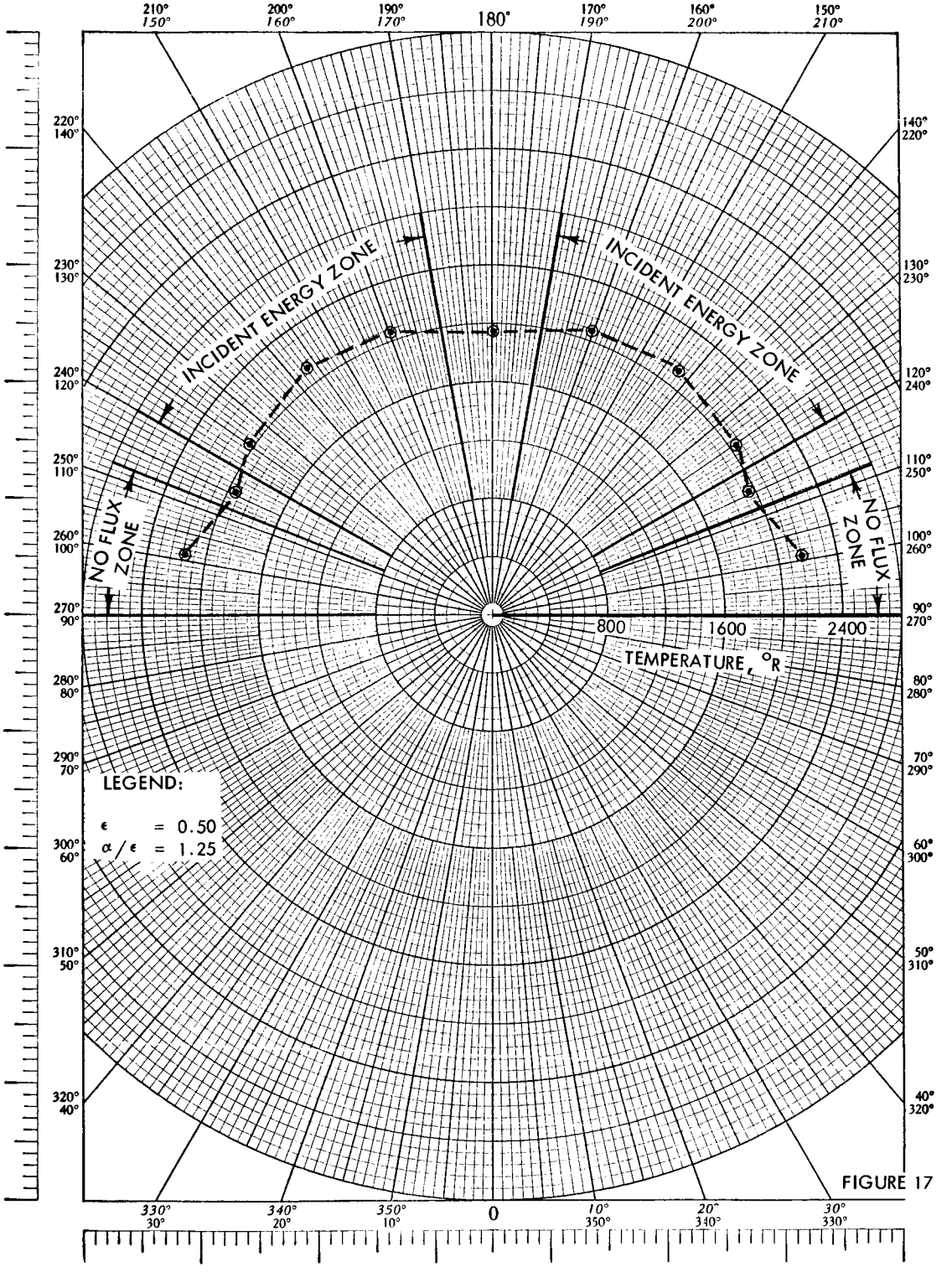

FIGURE 17

SOLAR TEST RIG CONSTRUCTION

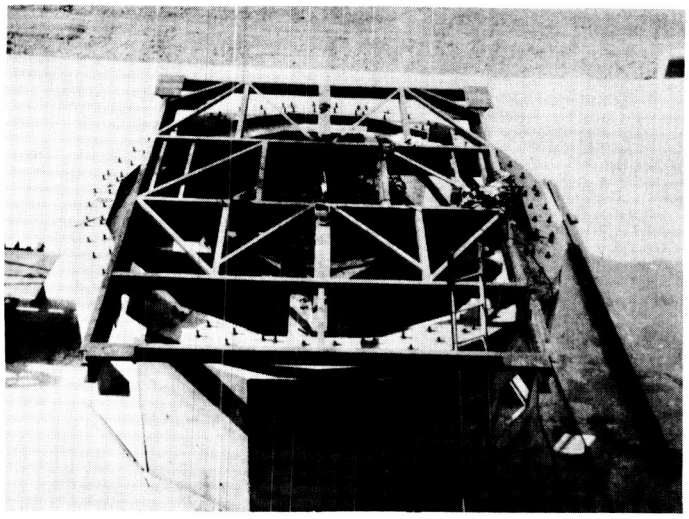

SOLAR TEST RIG FOUNDATION
AND UNDERCARRIAGE

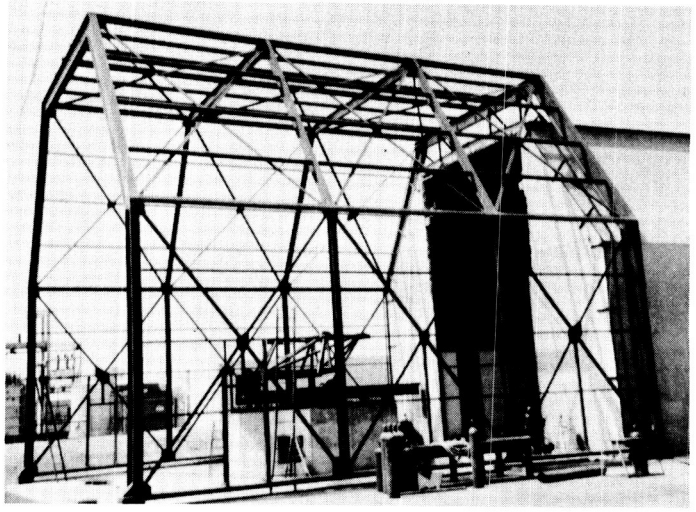

RETRACTABLE ENCLOSURE SUPERSTRUCTURE

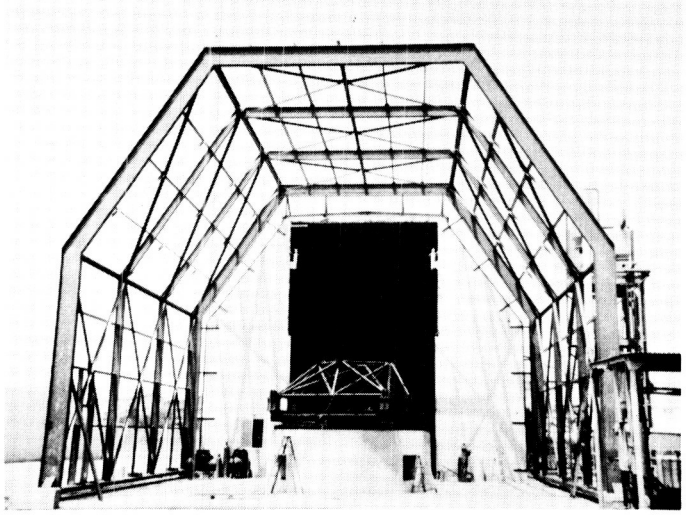

END VIEW OF ENCLOSURE AND
PCS SUPPORT ASSEMBLY

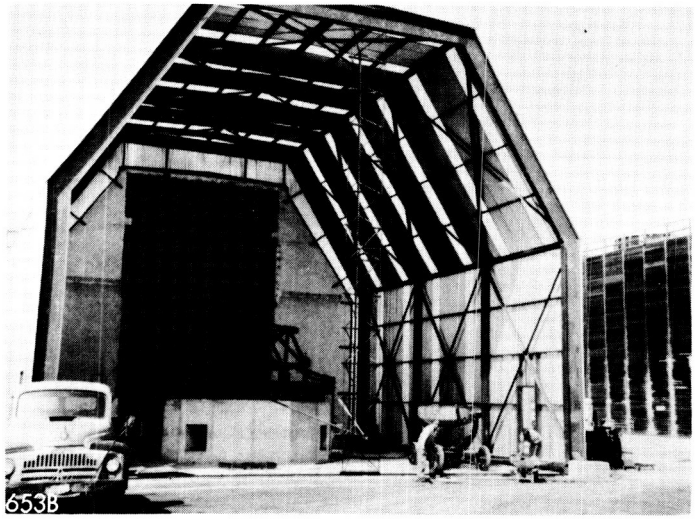

ENCLOSURE WITH SIDING COMPLETED

FIGURE 18

SOLAR TEST RIG

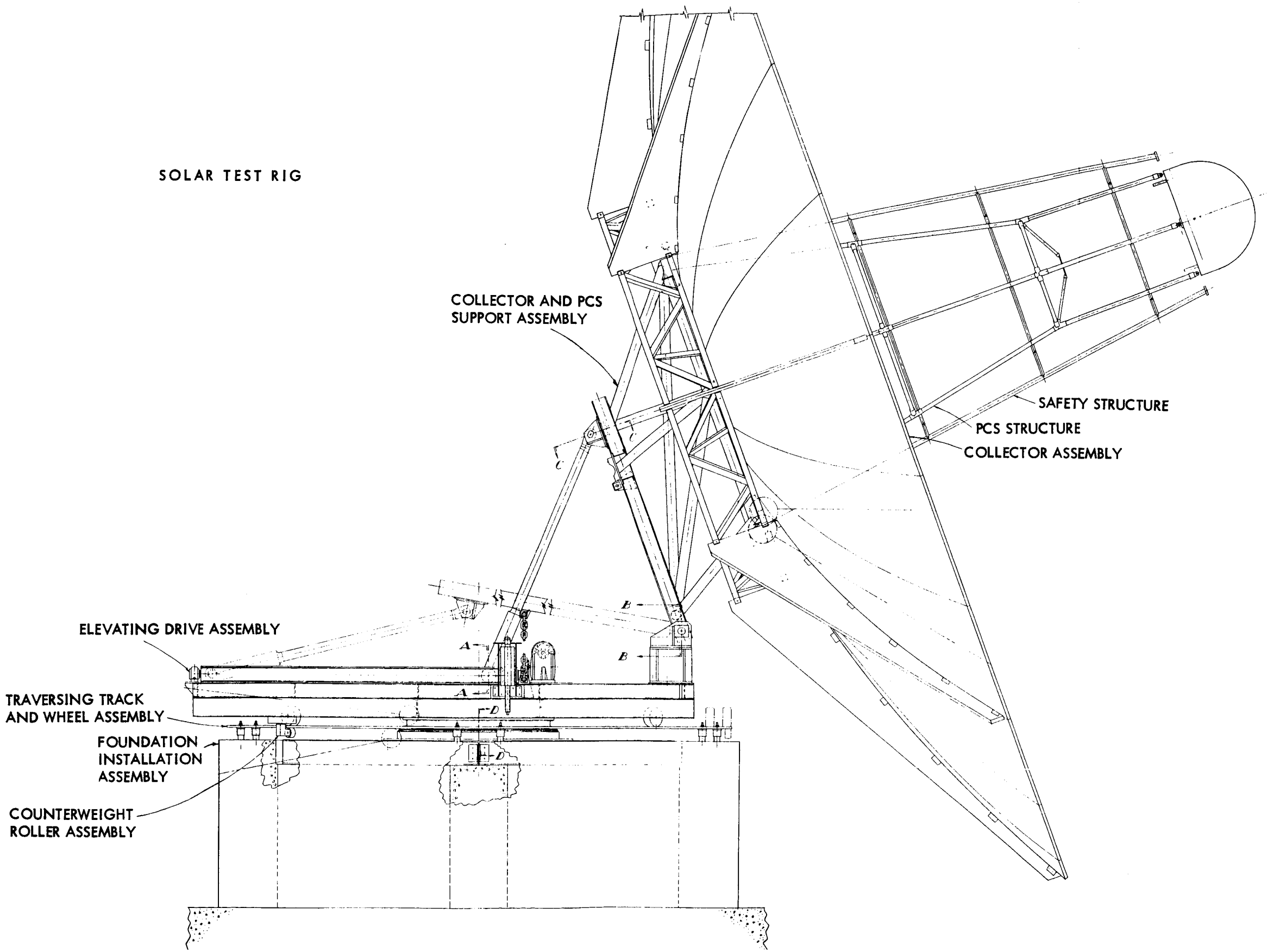

FIGURE 19

but will consist of a container for the storage and employment of inerting and quenching for emergency safing of the lithium hydride container. Provision will also be made for the actuation of shading elements to block the solar energy from the boiler/heat storage unit.

Specifications are being revised to obtain final quotes on the azimuth and elevation tracking and drive systems to be employed in the rig. These elements of the system will be retrofitted to the rig.

IV. CURRENT PROBLEM AREAS

As reported last quarter the most important current problem area remains the need to expedite component test activities in the development and acceptance test rig. Although performance in the test rig itself has been excellent, the pump difficulties have delayed the condenser, boiler and CSU component test schedules.

The difficulty encountered in the preprototype condenser-radiator has further delayed completion of the component test phases. It is now planned to reschedule a modified preprototype unit in the component test booth after completion of immediate boiler and CSU checkouts. In the interim, glass manifolded tube testing will be conducted to quantitatively evaluate tolerance to tube flow and thermal differences.

Components have been and will continue to be made available to the test laboratory personnel on a schedule insuring the availability of components for installation during test shutdown periods. In this way the full capacity of the single component test facility with its multiple booths will be gained.

V. PLANNED DIRECTION OF EFFORT FOR NEXT QUARTER

Modifications will be made to the preprototype condenser. These modifications will be based on analysis of current test results and on results of a glass manifolded breadboard test.

Testing of the preprototype No. 1 boiler will be completed in the argon inerted test booth. Fabrication of the second preprototype boiler will be completed and the third initiated. The design of the fourth boiler which will utilize thin Haynes 25 shells will be completed and fabrication started.

The final assembly and installation of the CSU in the test rig will be completed. Initiation of the CSU testing is dependent upon the duration of the boiler/heat storage testing. It is anticipated that the test initiation date for the CSU will be approximately the first of November.

The detail drawings for the power conversion system will be finalized early in the quarter and fabrication of the first PCS begun.

A detailed evaluation and stress analysis of the PCS under vibration environments will be conducted. The aim is to evaluate component mounting provisions and areas of potential weight reduction.

The test rig effort will consist of test planning and operation of component testing, ordering equipment for the system, ground checkout, and endurance test rigs. The C-210 installation will be completed and vibration testing of scaled fixtures conducted.

The solar collector activity will consist of completing the heavy duty backup panels for the solar test rig and fabrication of the first lightweight preprototype solar collector. Continued effort will be directed toward perfection of the aluminum vacuum deposition process. Various combinations of filaments, cleaning procedures, and vacuum conditions will be tried to obtain the most uniform and desirable coatings.

The movable shelter for the solar test rig will be completed during September. The calorimeter for solar collector testing will be fabricated and installed on the test rig. Completion of the solar test rig requires the purchasing and installation of the altitude and azimuth drive along with the automatic trailing system. The initiation of actual testing is expected during November or early December.

Testing of the preprototype control will continue and shall include operation at 125% of rated load and tests with an alternator-dynamometer. Environmental testing of components will be conducted and test results factored into the design of the second prototype unit. The first prototype control is to be fabricated and checked out by the first of December. Design efforts will include reducing the weight of the control by a repackaging design.

Corrosion test of capsules will be continued both in the argon and hydrogen atmosphere furnaces. Analysis of the seventh, eighth and ninth argon capsules and the second, third and fourth hydrogen capsules will be completed. Special capsule coating tests will continue.

The hydrogen diffusion study will consist of test on samples using the following special coatings: Nucerite and an A.O. Smith thick glass coating. Tests will also be conducted on tungsten samples and on FeCrAl samples of various thicknesses.

DISTRIBUTION LIST

	No. of Copies
National Aeronautics & Space Administration 801 Nineteenth Street, Northwest Washington 25, D. C. Attention: Walter Scott (DA)	1
National Aeronautics & Space Administration 1520 H Street, Northwest Washington 25, D. C. Attention: James Lazar (RPP)	1
Ames Research Center National Aeronautics & Space Administration Moffett Field, California Attention: Librarian	1
Goddard Space Flight Center National Aeronautics & Space Administration Washington 25, D. C. Attention: Milton Schach, Code 630, Bldg. NRL-101	1
Langley Research Center National Aeronautics & Space Administration Hampton, Virginia Attention: Emanuel Schnitzer	1
Langley Research Center National Aeronautics & Space Administration Hampton, Virginia Attention: Joseph Hallissy, Jr.	1
Lewis Research Center National Aeronautics & Space Administration 21000 Brookpark Road Cleveland 35, Ohio Attention: Richard P. Geye, SEPO	3 plus reproducible
Lewis Research Center National Aeronautics & Space Administration 21000 Brookpark Road Cleveland 35, Ohio Attention: Henry O. Slone, SEPO	1

DISTRIBUTION LIST (Continued)

	No. of Copies
Lewis Research Center National Aeronautics & Space Administration 21000 Brookpark Road Cleveland 35, Ohio Attention: Librarian	1
Marshall Space Flight Center National Aeronautics & Space Administration Huntsville, Alabama Attention: George C. Bucher, Code RPD	1
Marshall Space Flight Center National Aeronautics & Space Administration Huntsville, Alabama Attention: Josef F. Blumrick, Code S & MD	1
AiResearch Manufacturing Division The Garrett Corporation Phoenix, Arizona Attention: William Bowler	1
Allison Division General Motors Corporation Indianapolis 6, Indiana Attention: T. F. Nagey	1
Advanced Research Projects Agency Room 3E 153, The Pentagon Washington 25, D. C. Attention: Dr. Urner Liddell	1
Chance Vought Aircraft, Inc. P. O. Box 5907 Dallas 22, Texas Attention: Thomas Dolan	1
Convair-Astronautics 5001 Kearny Villa Road San Diego 11, California Attention: Krafft A. Ehricke	1

DISTRIBUTION LIST (Continued)

	No. of Copies
Electro-Optical Systems, Inc. 125 N. Vinedo Avenue Pasadena, California Attention: James H. Fisher	1
Air Force Systems Command Aeronautical Systems Division Flight Accessories Laboratory Wright Patterson Air Force Base, Ohio Attention: George W. Sherman	1
Air Force Systems Command Aeronautical Systems Division Flight Accessories Laboratory Wright Patterson Air Force Base, Ohio Attention: Donald Mortel	1
General Electric Company Missile & Space Vehicle Department 3198 Chestnut Street Philadelphia 4, Pennsylvania Attention: Edward Ray	1
Institute for Defense Analysis Universal Building 1825 Connecticut Avenue, N. W. Washington 9, D. C. Attention: N. W. Snyder	1
Jet Propulsion Laboratory California Institute of Technology Pasadena, California Attention: Garth E. Sweetnam	1
Jet Propulsion Laboratory California Institute of Technology Pasadena, California Attention: Librarian	1
Lockheed Missile & Space Division Sunnyvale, California Attention: Charles Burrell	1

DISTRIBUTION LIST (Continued)

	No. of Copies
Pratt & Whitney Aircraft 400 Main Street East Hartford 8, Connecticut Attention: William Podolny	1
Space Technology Laboratories P. O. Box 95001 Los Angeles 45, California Attention: George E. Mueller	1
Sundstrand Denver 2480 W. 70th Avenue Denver 21, Colorado Attention: Robert Boyer	1
Air Force Systems Command Ballistic Systems Division Inglewood, California Attention: WDAT-60-886-6/Mrs. Sangonard/3039	1
U.S. Army Signal Research Development Laboratory Fort Monmouth, New Jersey Attention: Arthur Daniel	1
Aerojet General Corporation Azusa, California Attention: Paul I. Wood	1
Atomics International P. O. Box 309 Canoga Park California Attention: Chief Librarian, 61-AT 2612	1
Boeing Airplane Company Aero-Space Division Seattle 24, Washington Attention: John S. Miller, 2-5454, Mail Stop 19-12	1
Atomics International P. O. Box 309 Canoga Park, California Attention: Joseph Wetch	1

DISTRIBUTION LIST (Continued)

	No. of Copies
Project Analysis Section General Electric Research Lab. P. O. Box 1088 Schenectady, New York Attention: V. C. Wilson	1
Project Analysis Section General Electric Research Lab. P. O. Box 1088 Schenectady, New York Attention: W. Adair Morrison	1
Griscom Russell Co. Massillon, Ohio Attention: Robert Schroeder	1
Lewis Research Center National Aeronautics & Space Administration 21000 Brookpark Road Cleveland 35, Ohio Attention: Bernard Lubarsky	1